AD-A038 527 AIR FORCE INST OF TECH WRIGHT-PATTERSON AFB OHIO SCH--ETC F/G 14/2
THE ELECTROSTATIC SENSING OF SIMULATED MA-1A GAS PATH DISTRESSE--ETC(U)
DEC 76 R W DUNN

UNCLASSIFIED AFIT/GNE/PH/76-2 NL

1 OF 1
ADA038527

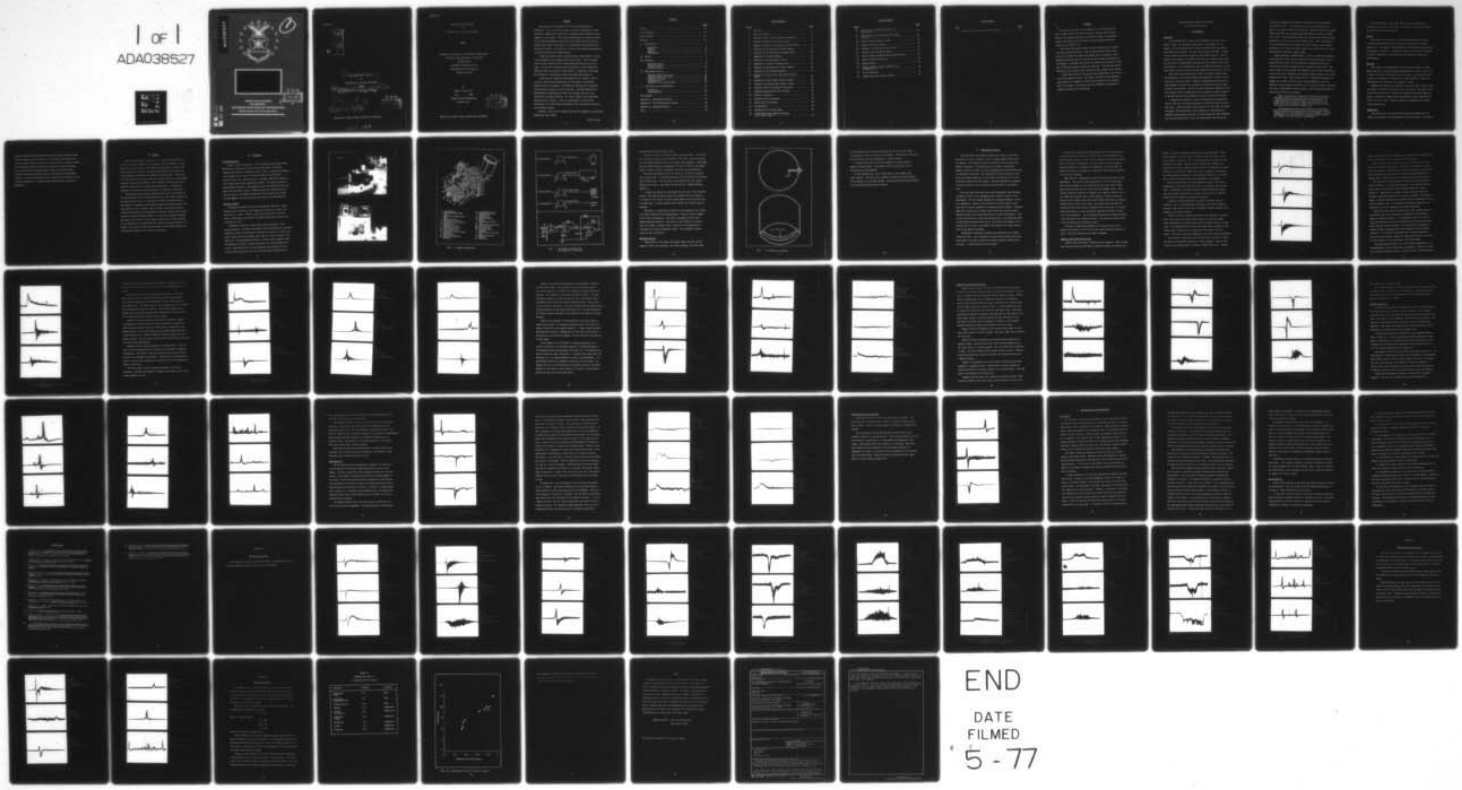

END

DATE FILMED
5-77

B.S.

UNITED STATES AIR FORCE
AIR UNIVERSITY

AIR FORCE INSTITUTE OF TECHNOLOGY

Wright-Patterson Air Force Base, Ohio

GNE/PH/76-2

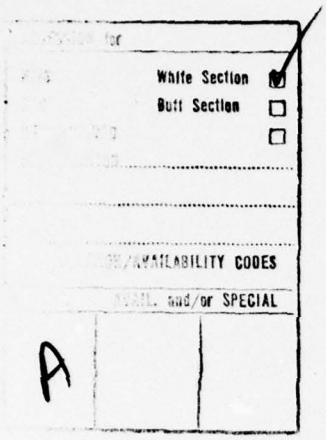

THE ELECTROSTATIC SENSING OF SIMULATED MA-1A GAS PATH DISTRESSES

THESIS

AFIT/GNE/PH/76-2

Robert W. Dunn
Capt USAF

Master's thesis

Dec 76 77p.

Approved for public release; distribution unlimited.

GNE/PH/76-2

THE ELECTROSTATIC SENSING OF SIMULATED MA-1A GAS PATH DISTRESSES

THESIS

Presented to the Faculty of the School of Engineering

of the Air Force Institute of Technology

Air University

in Partial Fulfillment of the

Requirements for the Degree of

Master of Science

by

Robert W. Dunn, B.S.

Capt USAF

Graduate Nuclear Engineering

December 1976

Preface

This thesis was sponsored by the Air Force Flight Dynamics Laboratory. It is a part of a series of studies, dating back to 1970, designed to examine the possibility of detecting metal particles in the exhaust of a jet engine. It has been estimated that at least 50 percent of the engine components in the gas flow emit metal particles prior to failure (Ref 14:58). The utility of a system that could predict these failures is obvious. This paper is a study of the detection capabilities of various electrostatic configurations.

I wish to sincerely thank my thesis advisor, Major Robert P. Couch, for his assistance and guidance during this project. Only his persistence has kept research alive on this phenomenon during the past few years. He initially formulated the vast majority of the concepts and approaches that were applied in this thesis. In addition, he designed the prototype of the Gaussian ring and the whole-body detectors.

I would like to express my appreciation to Mr. Claude R. Lynn Jr. of the Air Force Avionics Laboratory for his support in providing numerous pieces of equipment. The 4950 Test Wing was most cooperative and graciously provided the MA-1A start cart. The AFIT Department of Aero-Mechanical Engineering provided the building, facilities, and support for operating the MA-1A. Mr. John W. Parks of that department was particularly helpful. A note of appreciation is also due the technicians of the AFIT Physics Department, whose cooperation and advice were extremely helpful.

Finally, I would like to thank my wife and two daughters for patiently enduring my tour at AFIT.

Robert W. Dunn

Contents

List of Figures

List of Figures

List of Tables

Abstract

Jet engine distresses were simulated using a MA-1A start cart. Three primary methods were used to distress the gas turbine engine. Material was ingested through the compressor intake, the compressor section was rubbed with an aluminum rod, and foreign material was burned in the combustor can.

The current wave forms created by these distresses were observed with four separate detectors. Since the MA-1A was on rubber tires, the current between the chassis and ground could be measured. This chassis current was equal to the rate at which charge was expelled in the exhaust. A Gaussian ring around the exhaust port provided a second way of detecting charges leaving the start cart. The third and fourth devices were an ion probe and a screen that were placed in the exhaust.

It was found that the ring current was proportional to the derivative of the chassis current. The charges recorded by these detectors were noted to be dependent on the net charge present in the exhaust prior to distress. The charges were also dependent on the amount of material introduced by the distress.

THE ELECTROSTATIC SENSING OF SIMULATED MA-1A GAS PATH DISTRESSES

I. Introduction

Background

On 16 November 1970, Captain Robert Vapalensky as a part of his Master's thesis was conducting experiments on the plasma in a jet exhaust. As he was monitoring I/V traces, numerous very large amplitude spikes were observed. The next day the spikes increased. A check of the electronics system indicated it was working properly. On the morning of 18 November, the engine failed due to a broken turbine blade. All the normal instrumentation indicated that the engine had been working properly. It was hypothesized that the spikes were caused by micron sized metal particles given off as the turbine blade failed (Ref 13:1-2).

Since the spiking appeared well before the turbine blade failed, the monitoring of jet engine exhausts gave promise of a method for the detection of engine distress. Numerous investigations were made after 1970 designed to exploit the possibility of predicting engine failure through such monitoring. An Air Force Aero Propulsion Laboratory report and a General Electric engineering study indicated at least 50 percent of gas path failures were preceded by particle emission (Ref 14:58).

A summary and evaluation of these investigations was prepared by the Air Force Aero Propulsion Laboratory at Wright-Patterson Air Force Base, Ohio. After tracing the studies made up to June 1974, the report concluded, "The electrostatic probe technique for the detection of particles emitted during distress of turbine engine gas path components has not been demonstrated to have the effectiveness and reliability

necessary for advanced development or application in the foreseeable future" (Ref 11:17). One further quote from this publication was, "There is no question that an electrostatic probe will serve as a charged particle detector given suitable electronics and good signal to noise" (Ref 11:14). The attempts made until June 1974 had been confined almost exclusively to the use of an electrostatic probe. Also, the majority of the investigations were looking for Trichel pulses or high energy discharges to the probe that could produce up to five volts into a characteristically terminated coaxial cable.

Another experiment, AFAPL-TR-74-41, using low impedance termination and looking for Trichel pulses concluded, "No confirmed cases of probe counts (Trichel pulses) due to detection of charged particles were recorded for distress simulated in this evaluation" (Ref 12:71). However, oscilloscope photographs that appeared in this report showed that when the cable was terminated in one megohm, negative spikes were clearly evident (Ref 12:46). These spikes were not of sufficient magnitude to trigger the counters with the coaxial cable terminated at 93 ohms. McDonnell Douglas Research Laboratories of St. Louis, Missouri, evaluated the body of experimental evidence related to the electrostatic probe up until March of 1975 and concluded:

> The 0.5 micro-second duration, positive and occasionally repetitive pulses in the electrostatic probe output are due to negative corona discharges known as Trichel pulses. The large potentials required to induce these pulses are very likely to be due to regions (clouds) of net positive electrical charge convected with the exhaust gas.
>
> The mechanisms producing such clouds are not understood. Finely pulverized particulate matter or spray charging of the injected fuel may be responsible for their formation. Possibly a combination of surface reactions involving charge transfer and boundary layer separation is instrumental.

The report further stated that, "The evidence investigated is sufficiently promising to recommend a long-term, low-level continuation of related research (Ref 14:78-79).

Purpose

The purpose of this thesis is to study the feasibility of using electrostatic detection systems to measure the quantity of material expelled in a jet exhaust. An examination of the detector responses will be attempted. However, it is beyond the scope of this thesis to present a detailed explanation of the mechanisms that initially cause these perturbations.

Approach

Four detectors were installed on the gas turbine engine of a USAF MA-1A start cart. The three primary detectors were a ring, a probe, and a system to measure the chassis current to ground. The fourth detector, a grid, was not studied in detail due to time limitations. Details on these systems are included in the equipment section.

Exhaust perturbations were induced by injecting small amounts, under four grams, of material in the gas flow of the engine. The material was introduced in three ways. Material was ingested through the compressor intake. Material was rubbed off on the compressor shaft immediately in front of the air intake. Finally, aluminum and magnesium were burned in the combustor can.

Organization

The sections that compose this thesis are the introduction, the theory, the equipment, the experimental, and the conclusion. The theory

section outlines the current hypotheses concerning the mechanisms that produce charges in the jet exhaust. The equipment section describes the gas turbine engine, the detection devices, and the recording systems. The experimental section presents the results of actual experiments. The conclusions and recommendations are made in the final section. Appendix A contains additional figures illustrating the experimental results. The patterns developed by the screen and a description of its use are in Appendix B. Charge per mass calculations are included in Appendix C.

II. Theory

There is considerable uncertainty as to the actual mechanism that creates the charges observed in jet exhaust. This uncertainty is illustrated by the conclusions of the McDonnell Douglas report quoted in the Introduction (Ref 14:78-79). The most current theory is the clouds of charge hypothesis advanced by the McDonnell Douglas report. This theory is a contention that there are regions of charge coming out of the exhaust composed of many small particles. These particles collectively carry or cause the charges that are observed by the detectors. No definitive statement of how these clouds are produced is provided in this report.

The pocket of charge theory advanced by Couch is an explanation of one possible method of cloud charging (Ref 3:6). This theory asserts that an engine distress such as a rub creates a pocket of charged material. This pocket is composed of metal particles and an associated plasma. The high mobility of the electrons tends to charge the particles negative leaving the associated ions predominantly positive. However, the overall charge of the pocket remains neutral. As the pocket progresses through the engine, the inertia of the particles causes them to strike portions of the engine and as a consequence they lose their negative charge. The charge on the overall pocket becomes positive as the excess electrons on the particles transfer to the frame of the engine.

III. Equipment

Gas Turbine Engine

Figure 1 shows the equipment. The gas turbine engine Model Number GTCE 85-15-1, manufactured by the Garrett Corporation, AiResearch Manufacturing Company of Arizona, is used. Figure 2 shows the components of the engine. This engine is the power plant for the USAF MA-1A pneumatic start cart. The engine has a two stage centrifugal compressor and a single-stage radial inward flow turbine. The engine operates at approximately 42,200 rpm. The exhaust velocity was measured using pitot probe scans and found to have a maximum velocity of approximately 190 feet per second. The exhaust temperature with the bleed valve closed was 450 degrees F and with the bleed valve open it was 950 degrees F.

Detection System

The detection system consists of four separate detectors. These detectors were connected to the chassis of the cart, to a probe, to a ring, and to a screen. Figure 3 shows the pictorial hook up of the system. Each device uses 60 feet of RG 62A coaxial cable rated at 13.5 picofarads per foot.

The MA-1A is mounted on rubber wheels which insulated it from ground potential. A Keithley Instruments 600 B Electrometer was connected between the cassis and the ground to measure the whole body current. Any excess charge leaving the exhaust would leave an opposite charge on the start cart. The electrometer provided a variable input impedance which was adjusted to develop a voltage appropriate for the recording device in use. Amplification for the other detectors was provided by three direct current amplifiers built by the Flight Dynamics Laboratory at

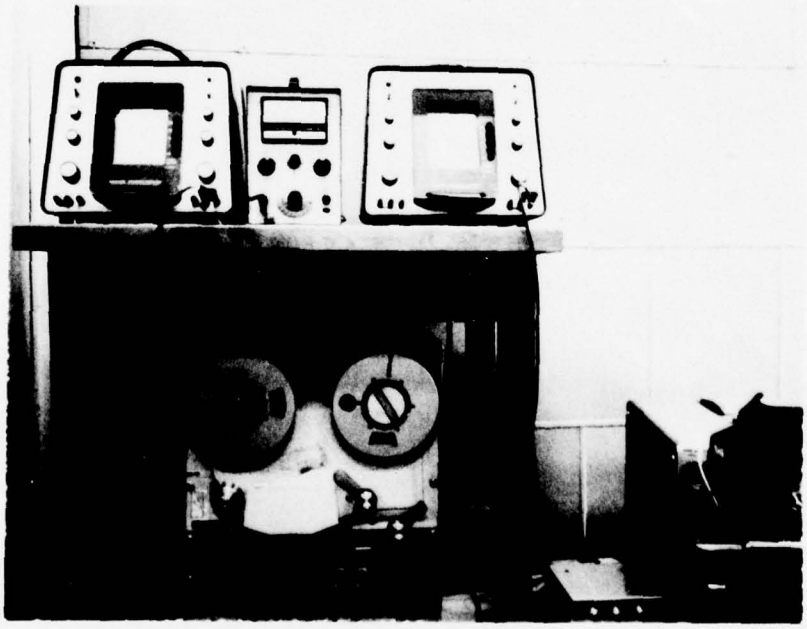

Figure 1 Equipment

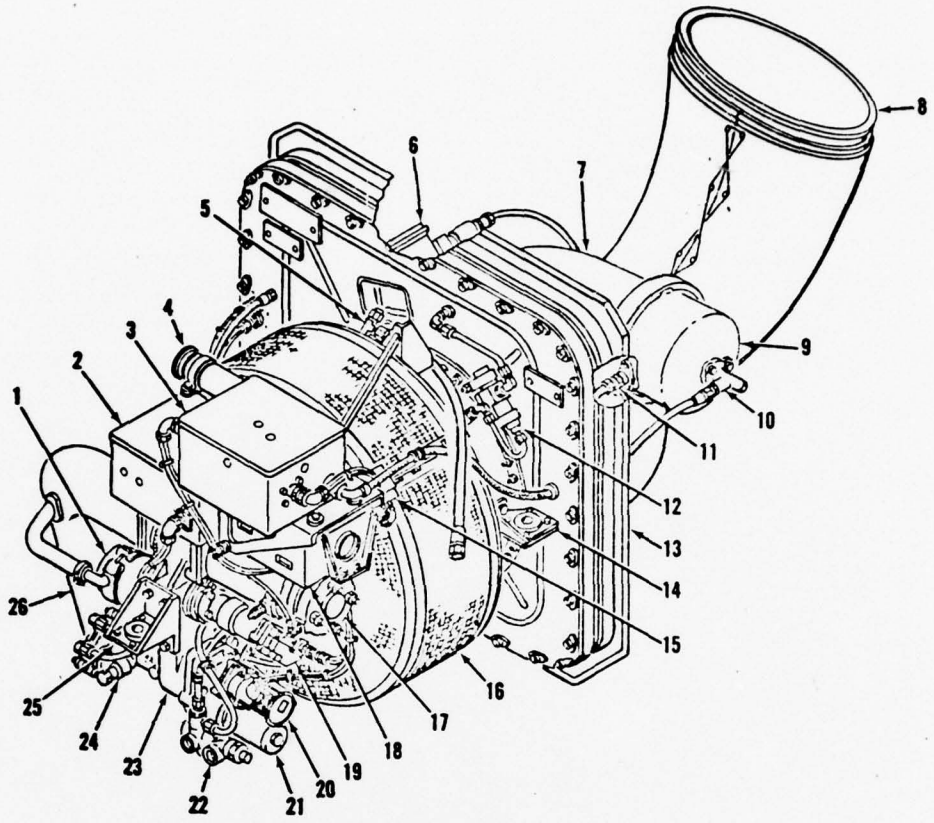

1. DC GENERATOR
2. GENERATOR REGULATOR ASSY
3. ELECTRICAL CONTROL BOX ASSY
4. RECORD CAN ASSY
5. OIL BREATHER FITTING
6. PNEUMATIC SHUTOFF VALVE
7. PLENUM ASSY
8. EXHAUST DUCT ASSY
9. COMBUSTOR CAP ASSY
10. FUEL ATOMIZER ASSY
11. IGNITER PLUG ASSY
12. DIFFERENTIAL AIR PRESSURE REGULATOR
13. BULKHEAD ASSY
14. RIGHT HAND MOUNTING BRACKET
15. OIL PRESSURE SWITCH
16. COMPRESSOR INLET SCREEN ASSY
17. STARTER ASSY
18. TIME TOTALIZING METER
19. CENTRIFUGAL SWITCH ASSY
20. TACHOMETER GENERATOR
21. OIL FILTER CASE
22. OIL PUMP ASSY
23. ACCESSORY DRIVE HOUSING
24. FUEL PUMP AND CONTROL UNIT
25. FORWARD MOUNTING BRACKET
26. DUCT ASSY

Fig. 2 Engine Components

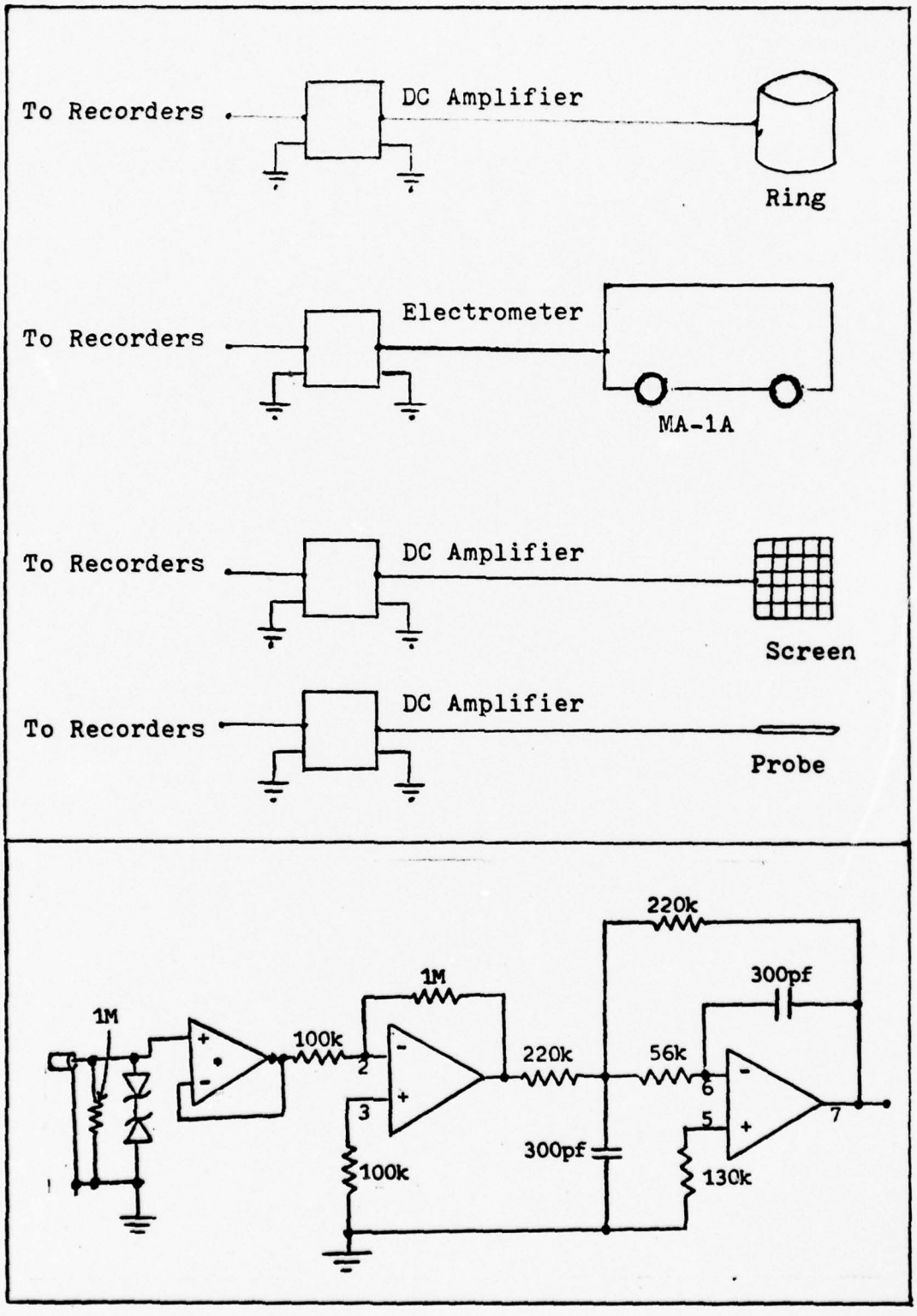

Fig. 3 Pictorial Diagram and
DC Amplifier Schematic

Wright-Patterson Air Force Base, Ohio.

Each direct current amplifier consists of two sections. One section has a gain of ten and an input impedance of 10^5 ohms. The other section is an isolated amplifier having a one megohm input impedance. Interchanging these sections allows an impedance of either 10^5 ohms or one megohm. Figure 3 shows a schematic diagram of the direct current amplifiers.

The ring was constructed out of a metal can 15 inches in diameter and 22 inches high. It was then bent into an oval 13 inches by 18 inches and 22 inches high. The oval shape was dictated by the oval exhaust opening of the MA-1A. The signal was fed into the 1 megohm isolation amplifier.

A second ring design was used during the last part of the experimentation. This ring was placed inside the original ring (see Figure 4). It consists of two strips of circuit board material two inches wide and 15 inches long. To help eliminate stray pickup, the original ring was grounded.

The probe is a sharp metal cylinder that is insulated from a stainless steel tubing and nut holding assembly. Figure 4 shows a diagram of the probe configuration. The probe is generally fed into the 1 megohm isolation amplifier. The screen or grid consists of nichrome wire .040 inches in diameter that is woven in 4 inch square over a 34 inches by 23 inches rectangular frame. It was mounted 42 inches above the top of the MA-1A.

Recording Devices

The pictures in this thesis were taken either directly from the engine or from a tape recorder. For direct readings, the delay sweep

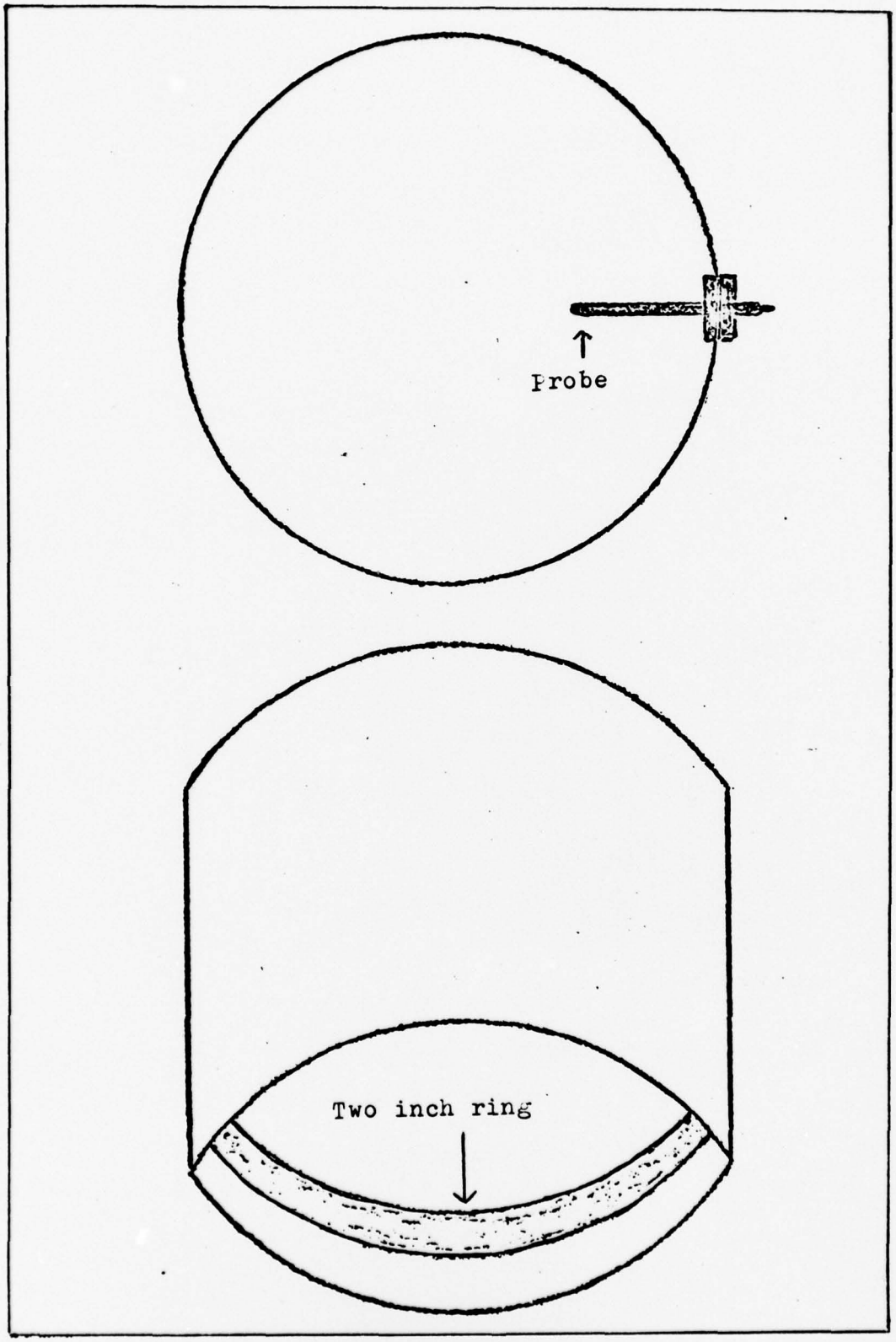

Fig. 4 Probe/Ring Assembly

on the Tektronix 549 storage oscilloscope was set to start at a time corresponding to when the engine was distressed. The storage circuit held the trace until it was photographed by a Polaroid camera.

A second method was to record the signals in an Ampex SP300 7 channel fm tape recorder. The signals could be played back into an oscilloscope and photographed.

A third approach was to use a Brush Mark II, two channel strip chart recorder. The strip chart recorder was hooked up either directly to the engine or to the tape recorder. By using two strip chart recorders, all four detection devices were observed.

IV. Experimental Results

The electrometer was connected between the chassis of the MA-1A and ground to obtain a measure of the net charge normally occurring to the exhaust. This charging current was found to vary inversely with ambient temperature. With the bleed valve closed, a fluctuating negative current of between 10 and 30 nanoamperes was observed depending on atmospheric conditions. This measurement implied that excess electrons were being transferred to the chassis and positive ions in turn were being expelled with the exhaust. This was confirmed by observing a positive current on the ion probe that was located in the exhaust flow.

With the bleed valve open the current measurements varied between a negative current of two nanoamperes and a positive current of two nanoamperes. The most common reading was a pulsating negative current of a nanoampere. However, the electrometer often fluctuated around zero and on occasion registered a pulsating positive current. Ingestion waveforms recorded when the whole body current was positive showed a marked difference from those taken when the current was negative. Some of this fluctuation in current was probably due to the modulating effect of the solenoid operated bleed valve. This valve was designed to continually vary air flow in accordance with feedback from engine sensors such as the exhaust thermostat.

Considerable aerodynamic turbulence was observed as the exhaust exited the MA-1A. This turbulence was noted with the bleed valve open and closed. The pressure profile was skewed decidedly forward and to one side. A definite swirl was also evident.

In most of the oscilloscope photographs used in this thesis, the vertical divisions are given in terms of current. This method of presentation was selected in order to give a basis for comparing the amplitude of the various photographs. The wide range of input impedances made the voltages too divergent for comparison. The values were obtained by dividing the voltage per centimeter by the voltage amplification and input impedance.

There were two configurations used for the probe and ring in these experiments. The initial design consisted of a ring 22 inches long. The probe was mounted in, but insulated from the ring. This arrangement placed the probe about 4 inches above the exhaust outlet. This ring was extremely sensitive to charges in the exhaust; however, due to its length the responses were a cross between a ring and a cylinder. There was also evidence that some of the charges were coming in physical contact with the sides of the ring. This charge contact further distorted the pattern that would be expected from a true ring. To correct these deficiencies, a second system was constructed and used in about 1/3 of the experiments. The new system grounded the old ring and placed a new ring inside the original container. The probe was moved up until it was 10 inches above the exhaust outlet.

The lack of sensitivity exhibited by the new ring due to its smaller area resulted in some of the ring signals being obliterated by noise. The probe response was virtually unchanged.

Ingestion with Bleed Valve Closed

Various types and amounts of materials were ingested. Their voltage wave forms were developed through an impedance between the detector and

ground. The actual quantities ingested were only approximate. These approximations were due not only to possible measuring error but also to the method of ingestion. The ingested material was poured into the compressor air intake. However, before reaching the compressor the material had to drop at least 18 inches and had to transverse two intake screens of 1/4 inch mesh. There was no way to assure all the material was sucked into the compressor. The ingestion process was also spread over a finite period that varied from experiment to experiment.

Most of the particles were sized through a screen. This sizing established an upper size limit but placed no constraints on the lower limit. Therefore, as the particles were conveyed through the engine, they were probably distributed in a manner that ejected the lightest particles first followed by the heavier particles.

A number of factors affected the ingestion patterns that were obtained. Some of the predominant influences, other than a change in material, were particle size, rate of ingestion, amount ingested, input impedance, and plasma polarity.

Figure 5 shows the patterns developed by the ingestion of approximately four grams of 50 micron nickel powder in a positive plasma. These photographs were taken directly from the engine using the storage scope. The patterns were not of the same event but were typical of the traces usually obtained by the ingestion of this amount of nickel powder. The first ring-probe configuration was used in these photographs.

As is shown in Appendix A, the probe can give a variety of traces. The probe is particularly sensitive to input impedance. Since it was located in the exhaust blast, a number of forces acted on it. Factors

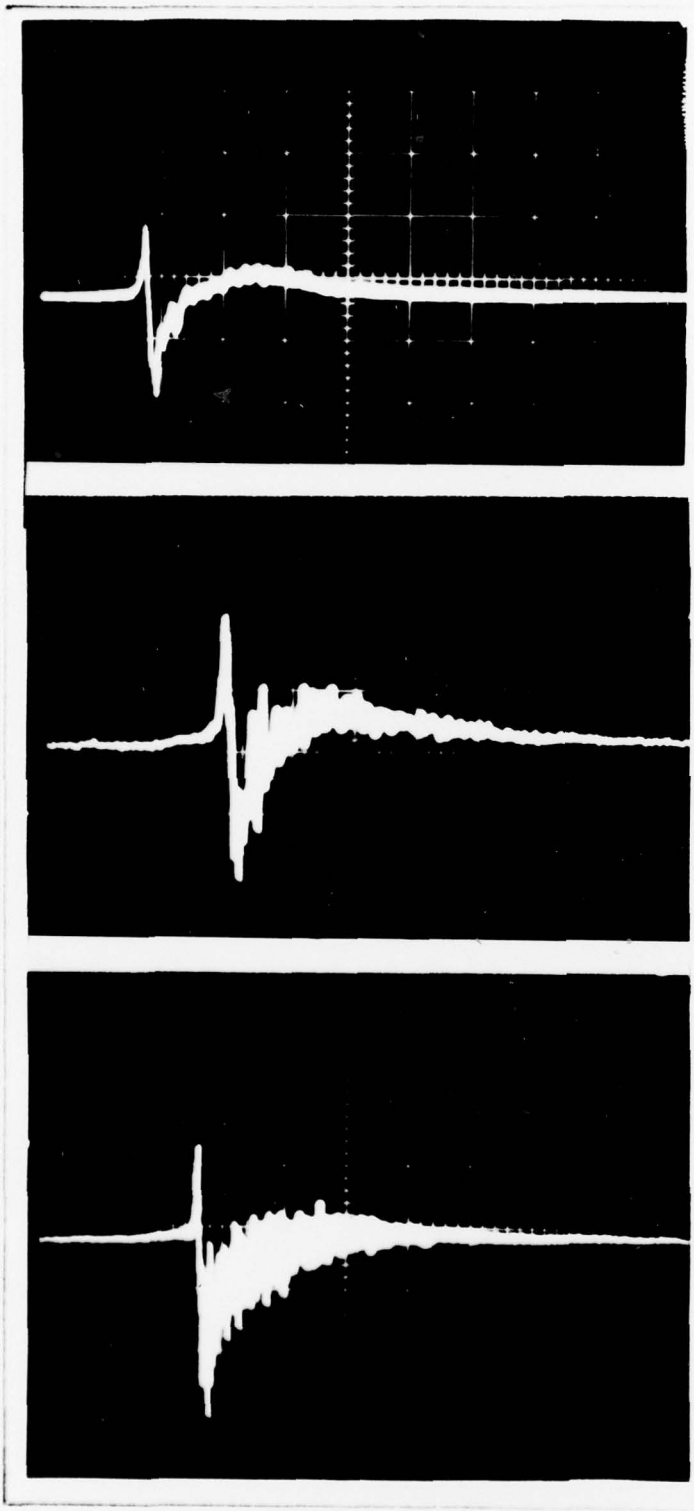

A.
Whole Body
(+ down)
0.4 S/cm
5.0 microamps/cm

B.
Ring
0.4 S/cm
0.5 microamps/cm

C.
Probe
0.4 S/cm
0.1 microamps/cm

Fig. 5 Ingestion of Three to Four Grams of Nickel Powder

such as temperature, dynamic buffeting, contamination, and biasing from contact with ions all could modify the probe response.

Figure 6, when compared to Figure 5, shows the effect of a mass change on the whole body pattern. In Figure 6, 0.5 grams of 50 micron nickel was ingested. The deletion of the lower spike on the whole body was a consistent occurrence once the amount ingested dropped below a certain level. This held for all the substances that were ingested.

The lower spike associated with the ingestion wave forms such as shown in Figure 5 is a transitory occurrence. The temporal nature of this pattern is illustrated by the sustained ingestions shown in Appendix A. Apparently, the negative charges associated with the particles temporarily suppress the positive ion charge. The negative charge on conducting particles is acquired from the attachment of electrons or negative ions. On insulators the negative charge can be a combination of contact charging and electron attachment.

Since this lower spike is related both to the ingestion mass and the particle size, some aerodynamic idiosyncrasy of the diverging nozzle is probably a factor. It is conjectured that as a cloud of plasma and particulate matter is expelled, the plasma ions slow down faster than the heavier particles. The particles are temporarily bunched together suppressing the plasma charge with their negative potential. It is further conjectured that very large conducting particles would discharge against the engine walls prior to exit and do not contribute to the development of the lower spike.

The ring design in Figure 6 is of the second configuration. It differentiated the whole body signal as predicted. However, the small area (60 square inches) created a detection problem. The photograph

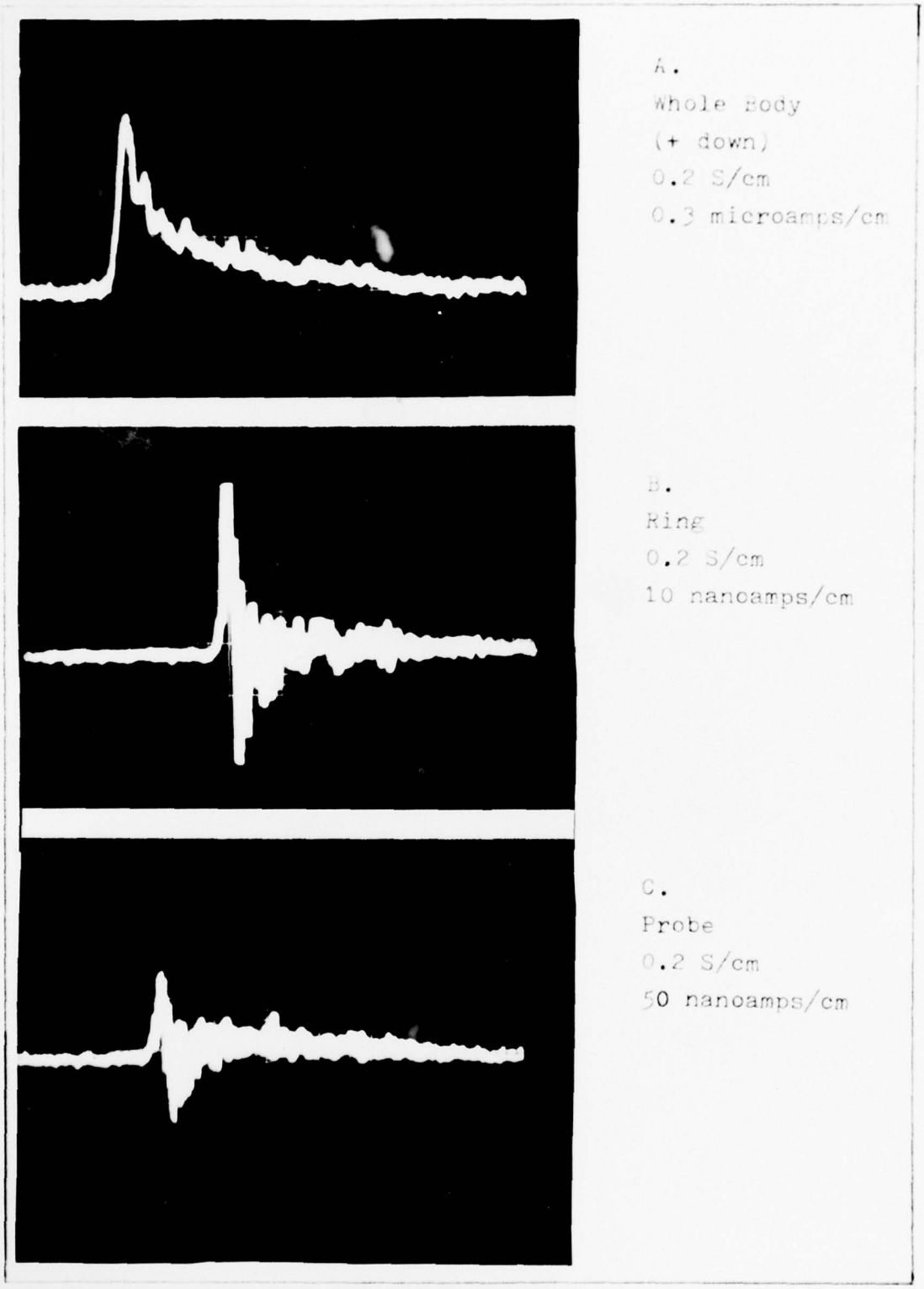

Fig. 6 Ingestion of One Half Gram of Nickel Powder

in Figure 6B was taken directly from the engine. The tape recorder was not used since the tape noise was close to the same magnitude as the signal.

One half gram of titanium was ingested in Figure 7. The whole body pattern shows a definite hump after the initial upward spike. This hump is probably due to the ignition of some of the titanium in the combustor can. The first spike on the ring trace is due to a random pulse the engine occasionally emitted. The titanium pattern is the second spike on the trace and was nearly obliterated by the tape noise. The two inch ring design was used in this figure.

Figure 8 shows the ingestion of two grams of graphite. Despite lump ingestions of better than six grams of graphite, the whole body pattern was consistently monopolar. This seems to confirm the lower spike in Figure 5 is not only related to the amount ingested but also to the particle size. Graphite showed the largest charge of any substance ingested. The ring used in Figure 8 was of the initial design and was used without amplification.

Figure 9 shows a typical ingestion of household flour. Flour was used to see if perturbations were introduced by ingesting a flammable nonconductor. The traces of the whole body and the ring have contours that are more irregular than graphite. However, this is speculated to be due as much to the coarseness of the particles as to the combustible nature of the flour.

The flour added a definite negative component to the probe responses. The additional negative component was evident in all of the probe responses to flour.

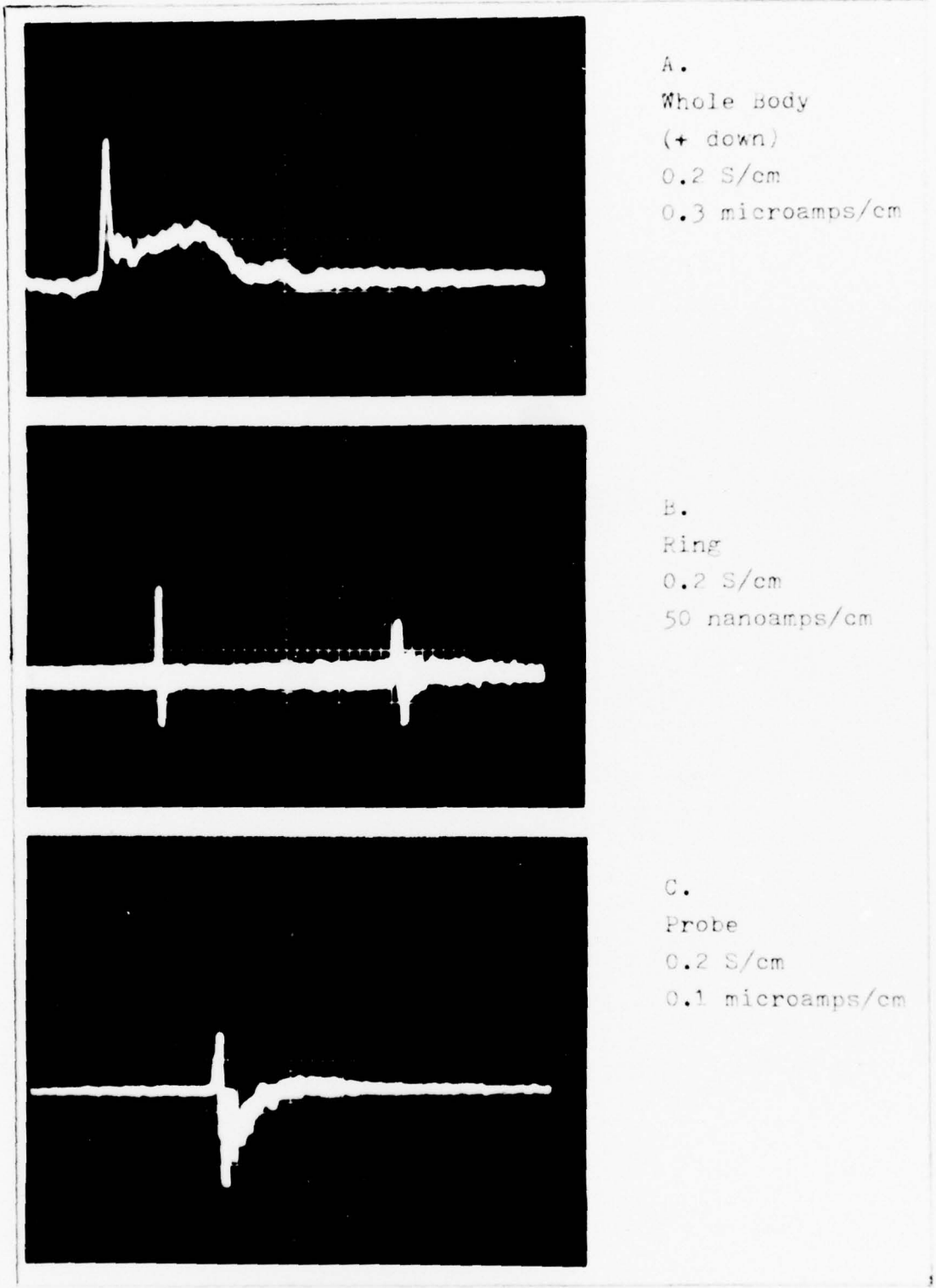

Fig. 7 Ingestion of One Half Gram of Titanium Powder

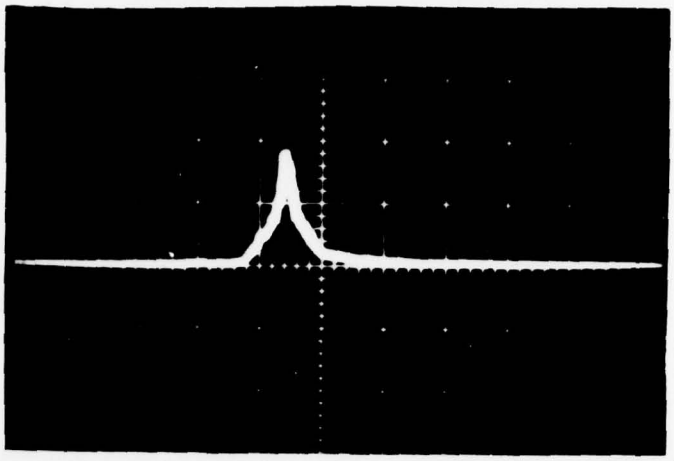

A.
Whole Body
(+ down)
0.2 S/cm
50.0 microamps/cm

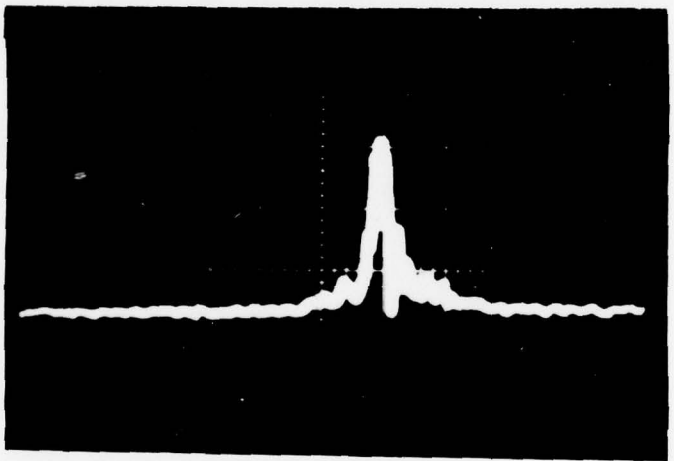

B.
Ring
0.2 S/cm
0.5 microamps/cm

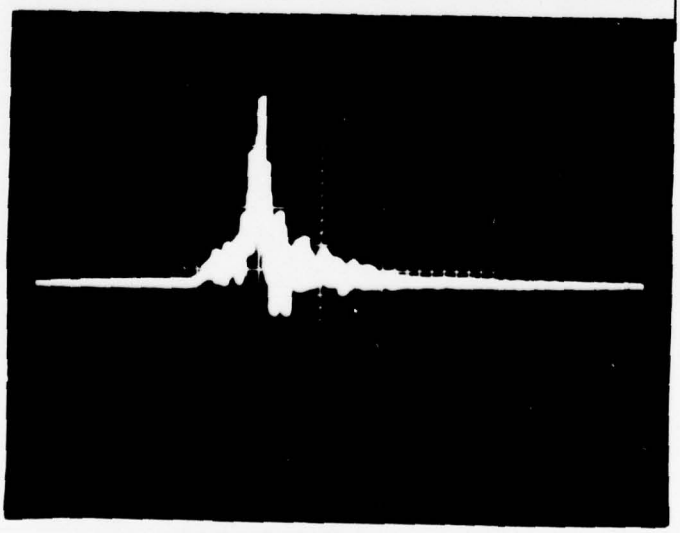

C.
Probe
0.1 S/cm
25.0 nanoamps/cm

Fig. 8 Ingestion of Powdered Graphite

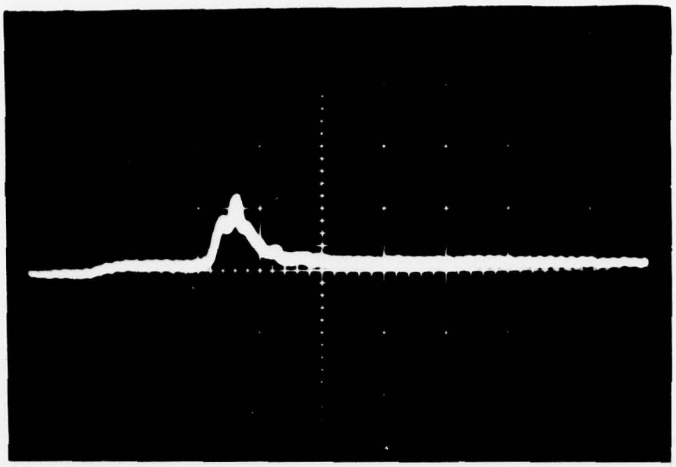

A.
Whole Body
(+ down)
0.1 S/cm
1 microamp/cm

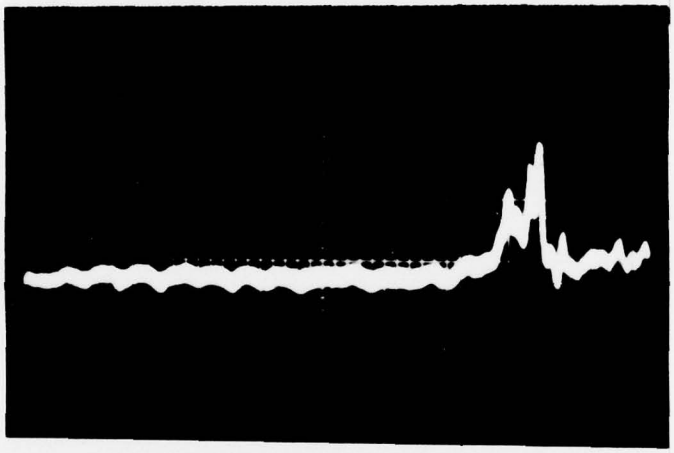

B.
Ring
0.1 S/cm
0.3 microamps/cm

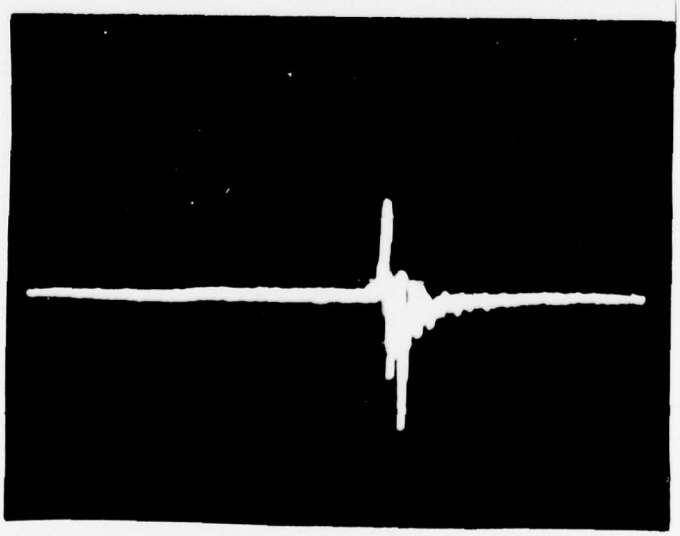

C.
Probe
0.1 S/cm
25.0 nanoamps/cm

Fig. 9 Ingestion of 250 Milligrams of Flour

Figure 10 illustrates the ingestion of approximately 2 grams of aluminum oxide powder. The negative portion of the whole body is mass related and can be eliminated by reducing the amount of material ingested. This waveform is very much like that of nickel. The main difference appears to be that the lower portion of the whole body is accentuated when compared to an equal amount of nickel. The 22 inch ring was used for this event. The trace in Figure 10B was taken without any amplification and was simply developed over a one megohm impedance. The sizable negative component in the exhaust was verified by the probe response.

Figure 11 was produced by the ingestion of less than a gram of finely ground quartz. No pronounced downward swing of the whole body signal occurred due to the amount ingested. A larger amount of quartz had previously produced a downward swing. The source of the smaller perturbation on the traces is unknown. The two inch wide ring was used in this figure.

In an attempt to see the effect of ingesting material in one cluster as opposed to the diffused ingestion of powdered materials, a 47 milligram buckshot was ingested. (See Figure 12.) The buckshot produced a relatively small perturbation. The whole body signal had to be developed over a 10 megohm impedance to make it distinguishable. It is questionable whether the buckshot was expelled from the engine. The charges picked up by the detectors were probably microscopic particles knocked off the engine or ions created by the impact of the buckshot. The 22 inch ring was used in this series.

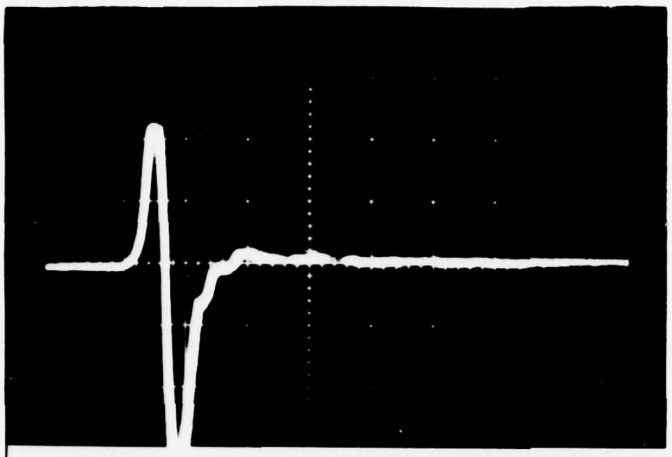

A.
Whole Body
0.1 S/cm
1.3 microamps/cm

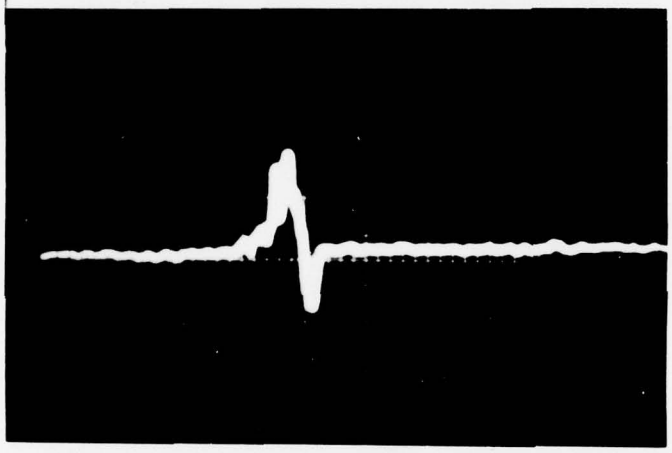

B.
Ring
0.2 S/cm
0.5 microamps/cm

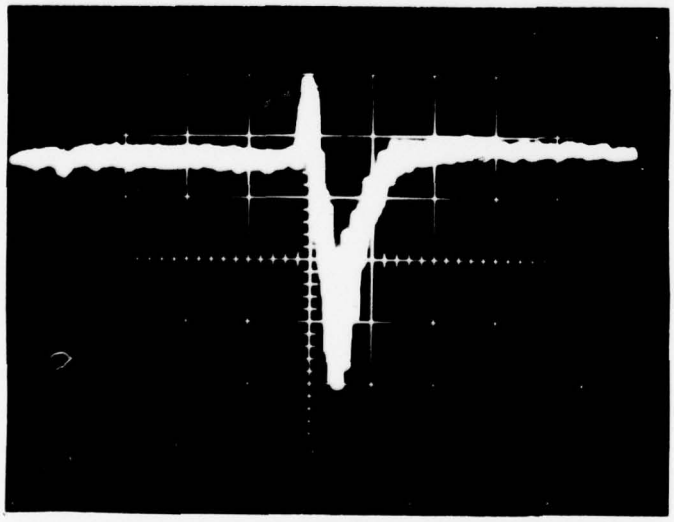

C.
Probe
0.2 S/cm
25.0 nanoamps/cm

Fig. 10 Ingestion of 2 Grams of Aluminum Oxide

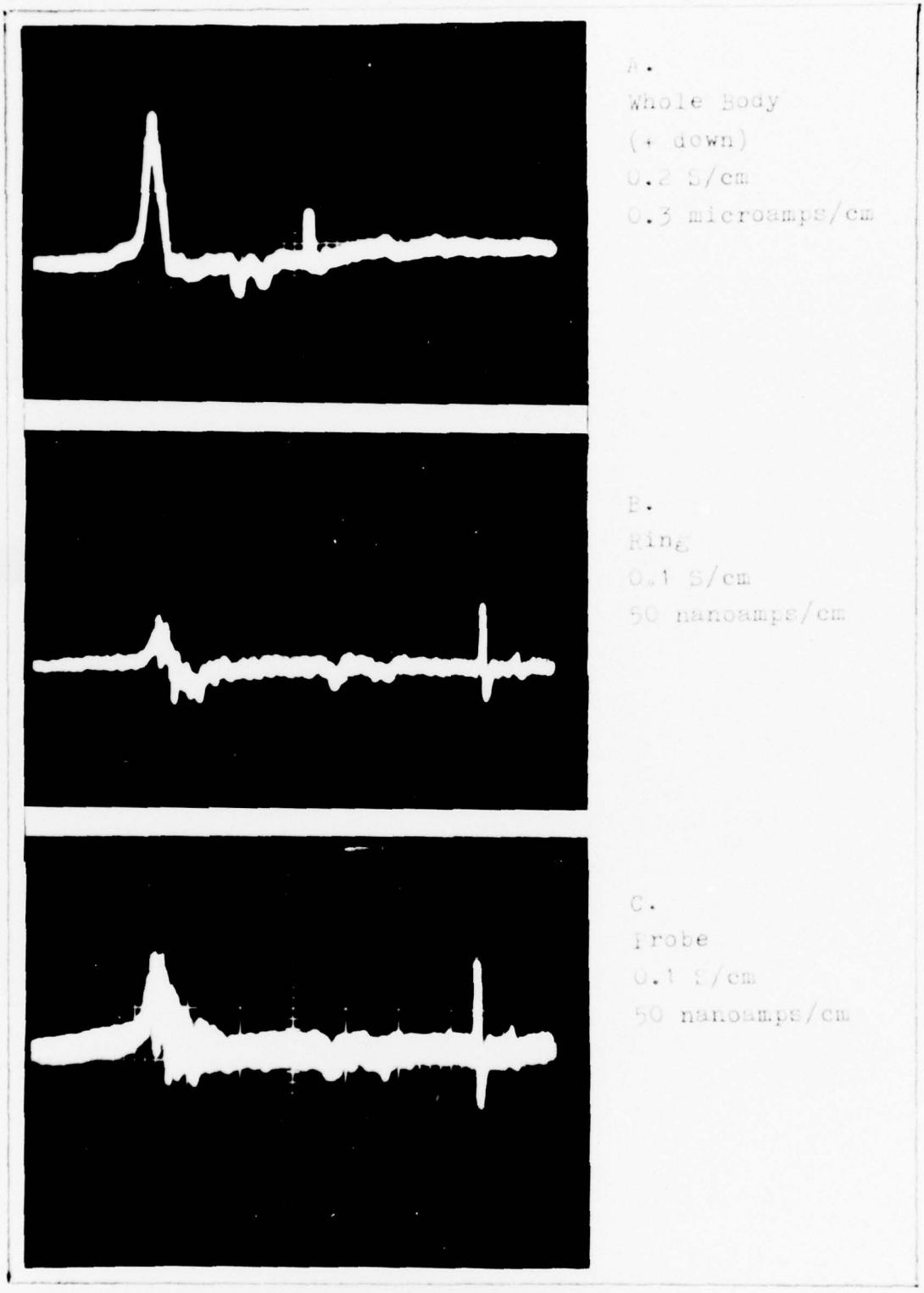

Fig. 11 Ingestion of Approximately 1 Gram of Quartz

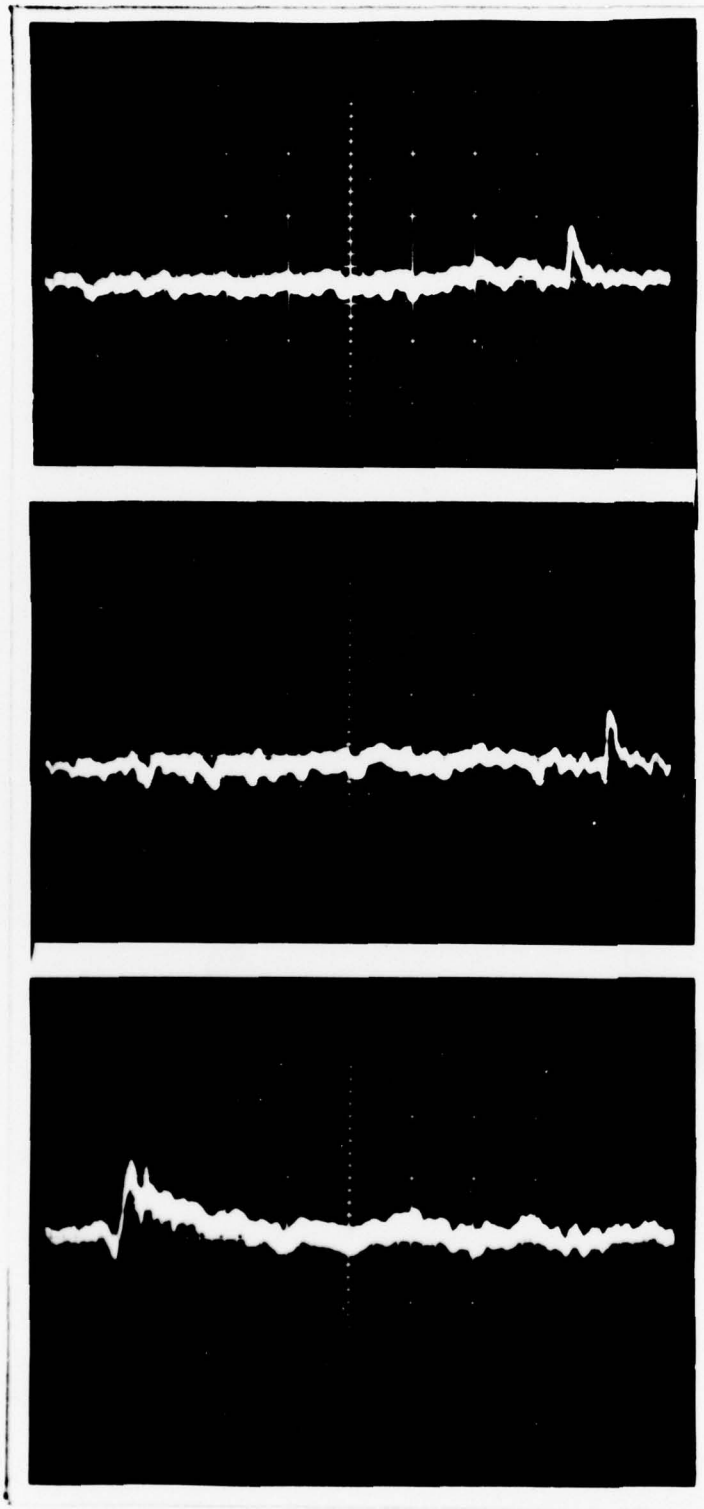

A.
Whole Body
(+ down)
0.5 S/cm
100 nanoamps/cm

B.
Ring
0.2 S/cm
100 nanoamps/cm

C.
Probe
50 mS/cm
10 nanoamps/cm

Fig. 12 Ingestion of a 47 Milligram Buckshot

Ingestions with Bleed Valve Open

Opening the bleed valve introduced several additional variables. On occasion the chassis current polarity switched from negative to positive. A positive whole body current implies a negative plasma. A difficulty in experimenting with the negative plasma was its transitory nature. When the bleed valve was open, a portion of the ingested material was vented through the bleed air port. A limited attempt was made to measure the output from the bleed air port with a ring. Sufficient time was not available to optimize the system and the only result was to detect small amounts of charged material exiting the bleed air port. The whole body signal would be expected to respond to both material expelled through the exhaust and through the bleed air port.

Figure 13 shows the ingestion of 50 micron nickel powder with the bleed valve open and a positive plasma. The probe signal did not develop over the noise.

Figure 14 shows the ingestion of 50 micron nickel powder into a negative plasma. The whole body traces show a marked departure from the traces taken in a positive plasma. The ring verified the alteration in shape. The probe signals did not develop above the noise. Appendix A shows some additional pictures of nickel and titanium ingested into a negative plasma.

Figure 15 illustrates two to three grams of aluminum oxide being ingested in a negative plasma. The patterns are either reversed or modified extensively from those obtained in a positive plasma. The ring used in this figure was 22 inches long.

Graphite and flour were also ingested in a negative plasma. They developed monopolar whole body traces with the polarity reversed from

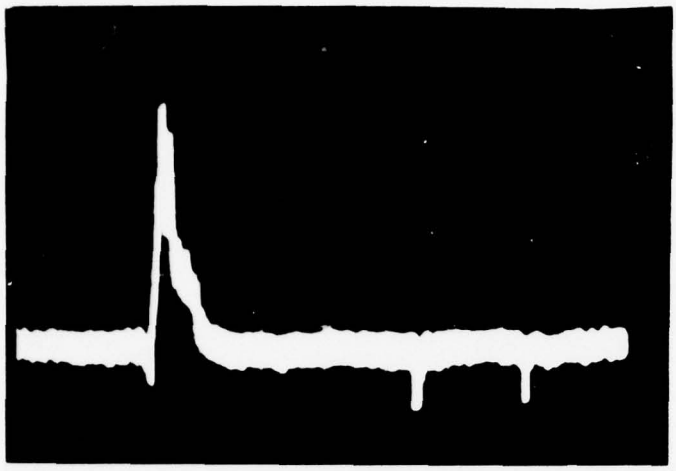

A.
Whole Body
(+ down)
0.5 S/cm
130 nanoamps/cm

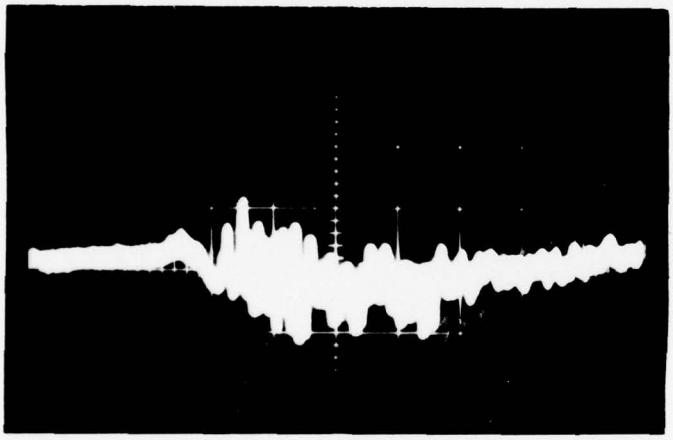

B.
Ring
0.1 S/cm
50 nanoamps/cm

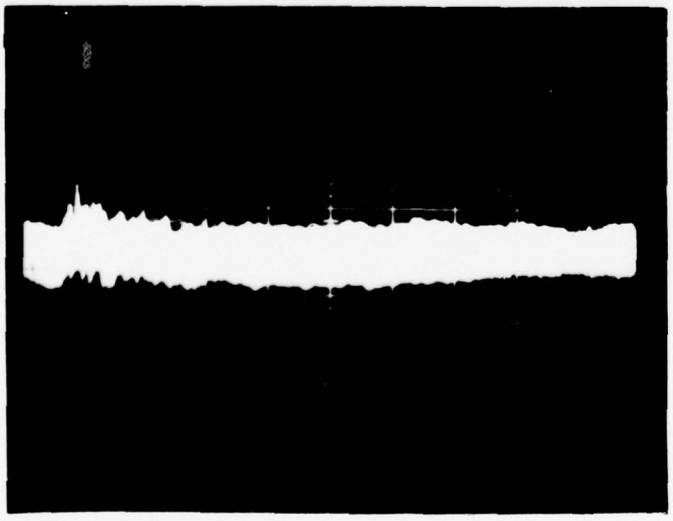

C.
Probe
0.2 S/cm
20 nanoamps/cm

Fig. 13 Ingestion of Nickel Powder
Bleed Open Positive Plasma

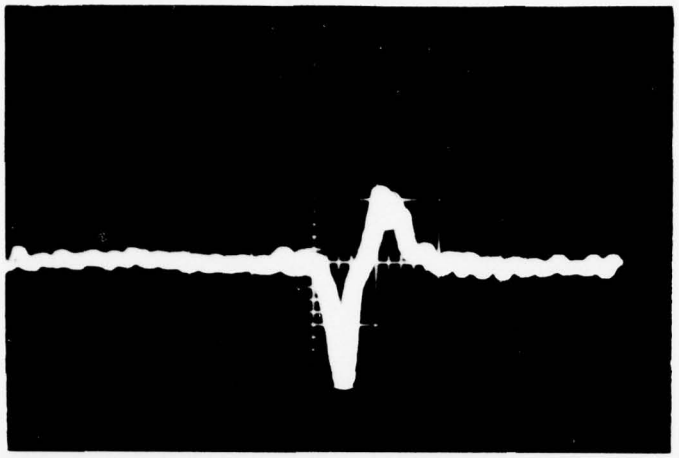

A.
Whole Body
(nickel)
(+ down)
0.1 S/cm
0.67 microamps/cm

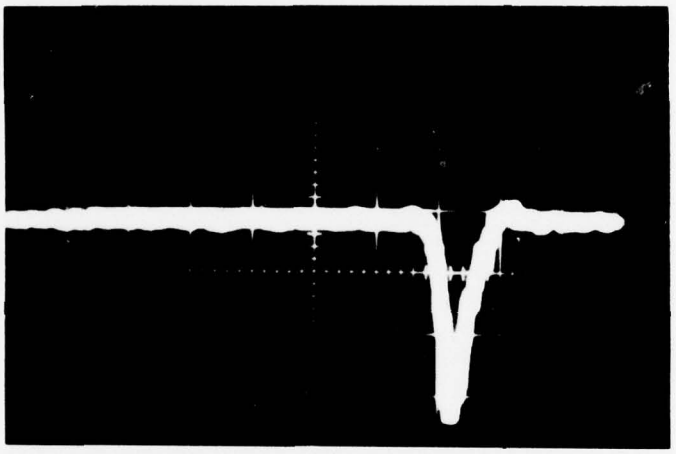

B.
Whole Body
(nickel)
(+ down)
0.33 microamps/cm
0.1 S/cm

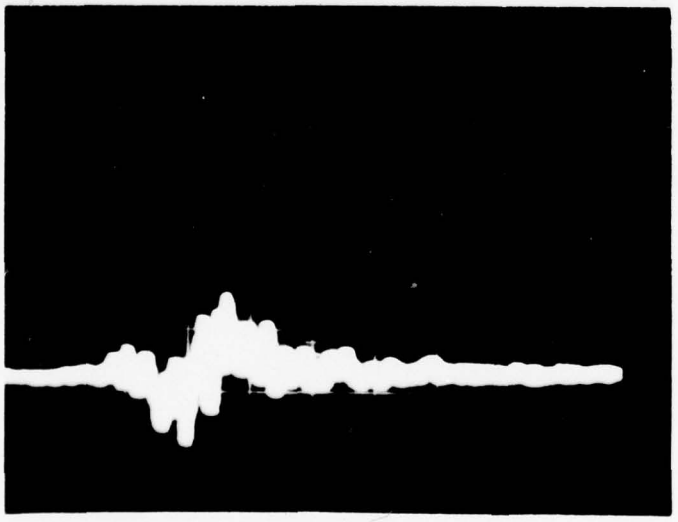

C.
Ring
(same event as B)
50 mS/cm
50 nanoamps/cm

Fig. 14 Ingestion of Nickel Powder
Negative Plasma

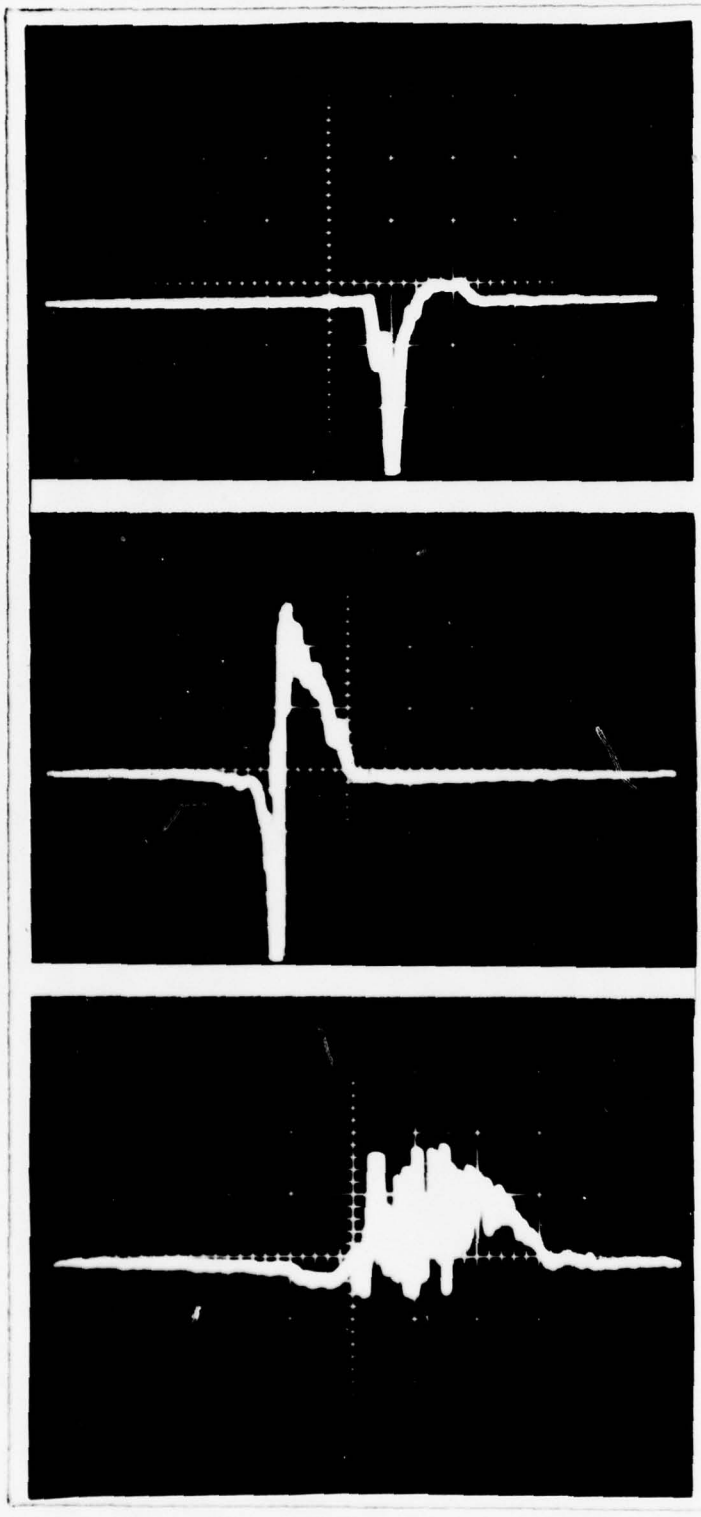

A.
Whole Body
(+ down)
0.1 S/cm
0.33 microamps/cm

B.
Ring
0.1 S/cm
0.3 microamps/cm

C.
Probe
50 mS/cm
50 nanoamps/cm

Fig. 15 Ingestion of Aluminum Oxide
Negative Plasma

that obtained in a positive plasma.

Only a limited number of pictures were obtained from negative plasma ingestion, since it occurred on a sporadic basis. The exact conditions that caused a negative plasma were never firmly established but cool damp days appeared to be a factor.

Combustor Can Burns

In order to accomplish this simulation, one of the bolts attaching the spray nozzle to the combustor can was removed. It was replaced by another bolt with a 3/32 inch hole drilled through the length of its shaft. The material to be burned was introduced through this hole. The materials burned in the combustor can were limited to aluminum and magnesium. This choice was dictated both by time constraints and the difficulty of achieving burns in the combustor can.

A burn of approximately 27 milligrams of pure magnesium strip is shown in Figure 16. The pure magnesium produced a significant charge. However, difficulties in getting the strip into the combustor can and insuring that it burned at the appropriate time led to the use of a 1/16 inch aluminum magnesium alloy welding rod.

The pattern developed by the welding rod is shown in Figure 17. The time duration is significantly longer with the addition of the aluminum. The aluminum tended to melt in drops of metal rather than to violently burn like pure magnesium. The magnesium in the rod appeared to splatter the aluminum producing a probe and ring signal that were not as sharply defined as either the pure magnesium or the pure aluminum.

Figure 18A illustrates the effect of melting 760 milligrams of aluminum. The last peak of Figure 18A is shown in Figure 18B.

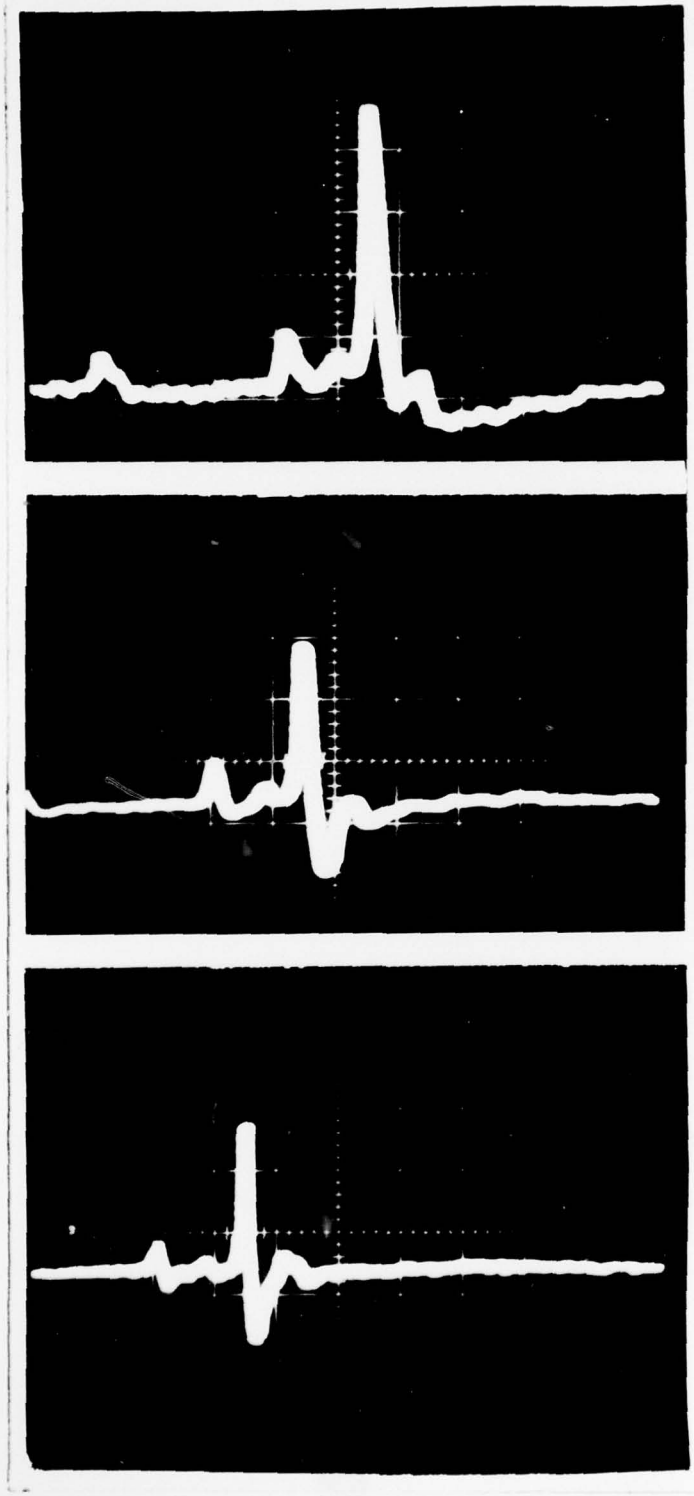

A.
Whole Body
(+ down)
50 mS/cm
0.3 microamps/cm

B.
Ring
50 mS/cm
0.1 microamps/cm

C.
Probe
50 mS/cm
0.1 microamps/cm

Fig. 16 Combustor Burn 27 Milligrams of Magnesium

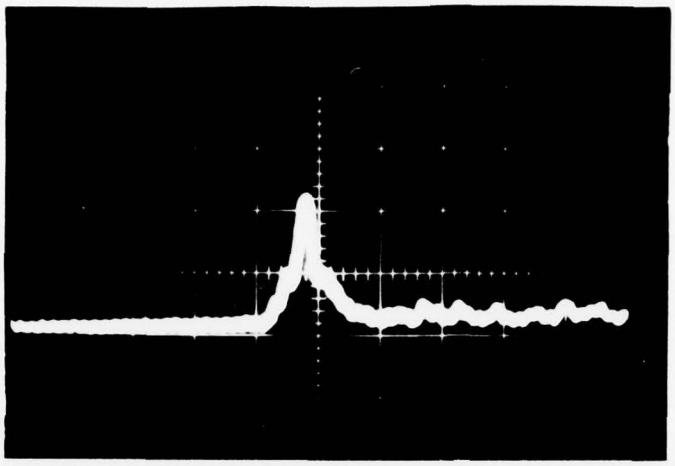

A.
Whole Body
(+ down)
0.1 S/cm
.06 microamps/cm

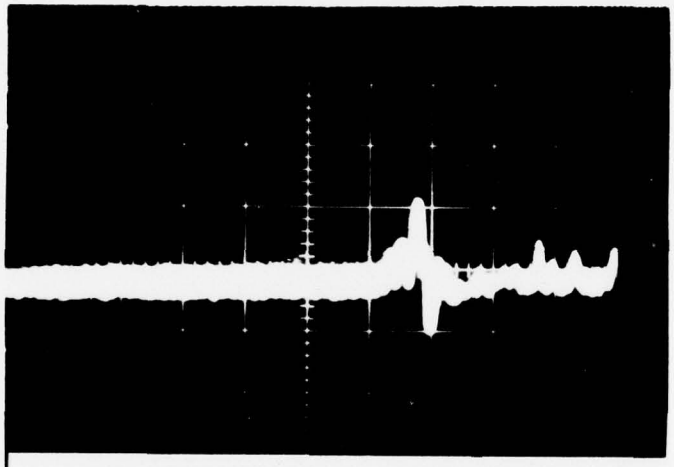

B.
Ring
0.1 S/cm
50 nanoamps/cm

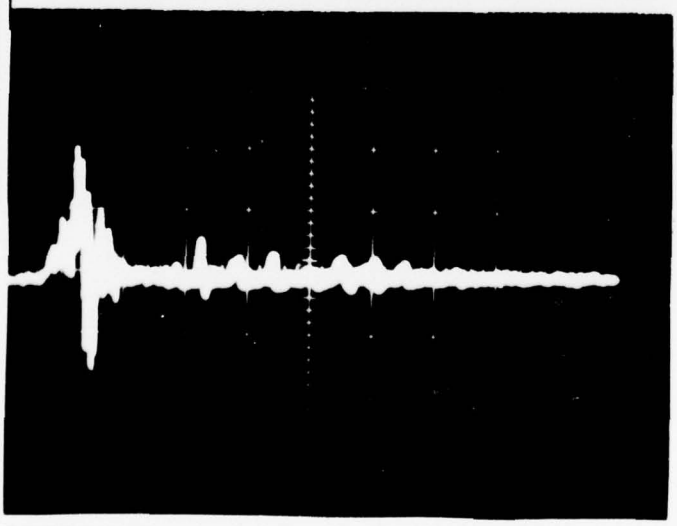

C.
Probe
0.1 S/cm
50 nanoamps/cm

Fig. 17 Magnesium Aluminum
Burn 620 Milligrams

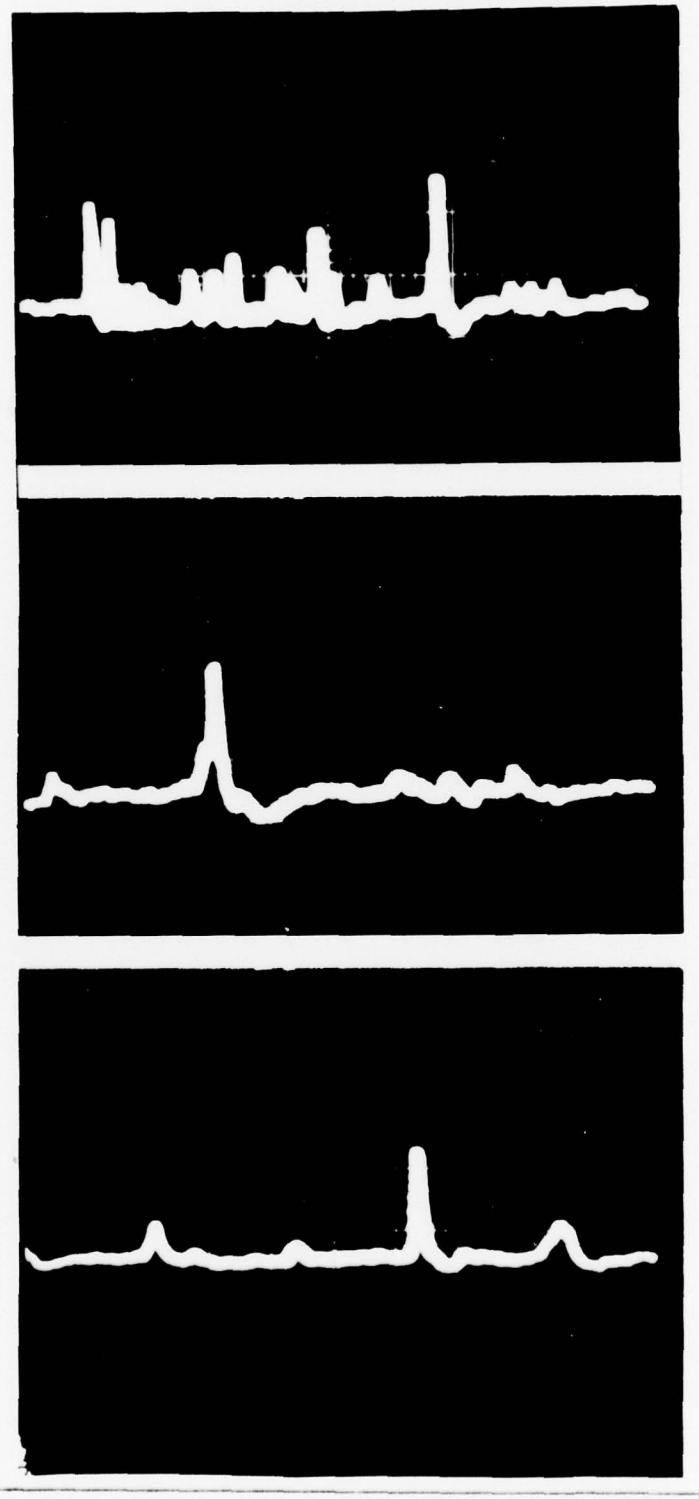

A.
Whole Body
(+ down)
10 megohm input
0.5 S/cm
67 nanoamps/cm

B.
Whole Body
(+ down)
(last peak)
0.2 S/cm
67 nanoamps/cm

C.
Ring
50 mS/cm
50 nanoamps/cm

Fig. 18 Melting of Aluminum

The response of the ring is shown in 18C. Figure 19A illustrates the response of the probe to melted aluminum.

When the bleed valve was open, it was possible to get two distinct patterns. One pattern agreed with the pattern established when the bleed valve was closed. The other pattern is displayed in Figures 19B and 19C. These are two separate photographs of the burning of approximately 586 milligrams and 637 milligrams of a magnesium aluminum rod in a negative plasma. The polarity of these burns appears to be reversed from that observed with a positive plasma.

Since the material was introduced next to the spray nozzle, some alteration of the spray pattern was introduced. What effect, if any, this had on the charging process is unclear.

Compressor Rub

The rub simulation was accomplished by rubbing a 1/4 inch aluminum rod against the compressor shaft immediately in front of the intake. Any metal ground off by this rubbing was sucked into the compressor. This method of distress was selected to preclude damage to the engine. However, there were several limitations to this approach. Rubs occurring in the internal section of an engine generally create a high temperature at the point of contact. The metal is usually gouged out as opposed to a sustained smooth grinding action. By rubbing the compressor shaft with a smooth aluminum rod, the amount of localized heating would be minimal.

For safety reasons, these rubs were created by pulling on a 30 foot cord and pulley arrangement. The maximum amount of metal ground

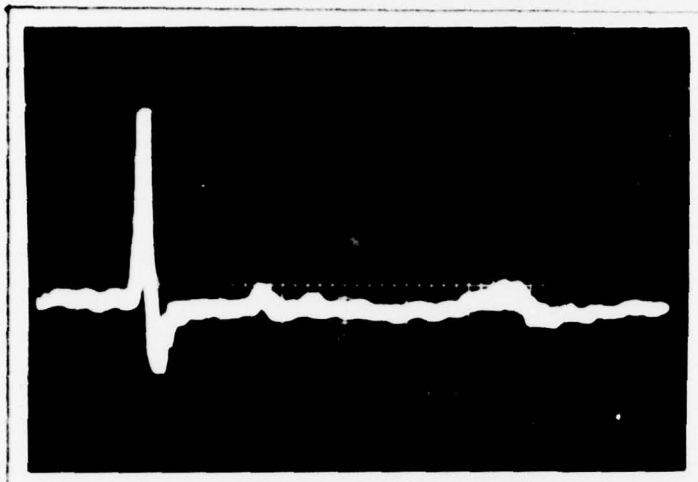

A.
Probe
(aluminum)
20 mS/cm
50 nanoamps/cm

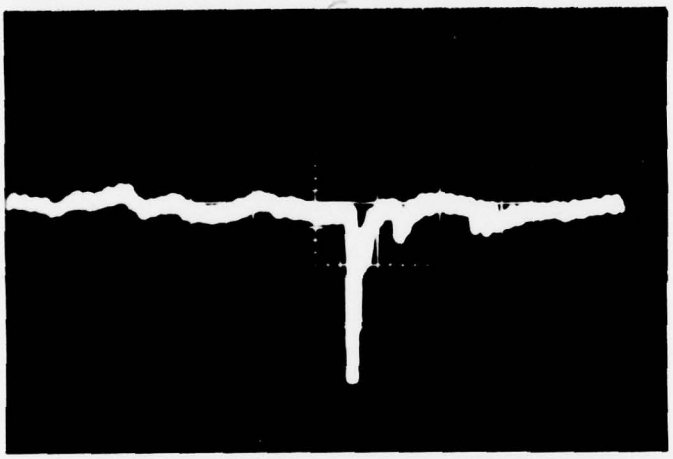

B.
Whole Body
(+ down)
Bleed Open
Magnesium-Alum
586 milligrams
0.1 S/cm
0.3 microamps/cm

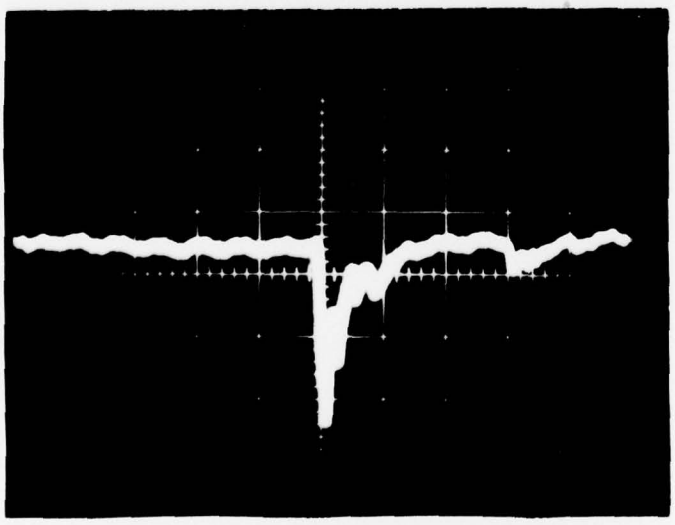

C.
Whole Body
(+ down)
Bleed Open
Magnesium-Alum
637 milligrams
0.1 S/cm
0.3 microamps/cm
(Tape 1/4 speed)

Fig. 19 Combustor Burn Photographs

off per rub in Figure 20B was estimated at between five and ten milligrams. A considerable variation in the amount of metal rubbed off was noted from one grind to another. The small amount of metal necessitated the use of between 10 and 100 megohms to develop the signal. At these impedance only broad shapes emerged due to RC time constants up to eighty milliseconds. The tape recorder was not used. All the photographs were independent events taken directly on the storage oscilloscope. Figure 20 shows three whole body photographs each created by pulling the aluminum rod against the compressor shaft. Figure 20A was developed over 10 megohms by pulling on a 60 pound test string. Three upward humps corresponding to three pulls on the string are barely discernable. In Figure 20B, a 3/8 inch rope was used and the impedance was raised to 100 megohms. The two rapid pulls on the rope producing two rubs are clearly discernable. In Figure 20C, the rope was again used and the impedance was dropped to 10 megohms. The initial upward hump corresponds to a single pull on the end of the rope. The perturbations toward the end of the sweep were fluctuations in the plasma current.

In Figure 21A, a ring photograph is shown with the electrometer set at 10 megohms. The single downward hump is barely discernable. Figure 21B shows a probe photograph taken at 100 megohms. Figure 21C is an ingestion of nickel at 10 megohms. The last figure demonstrates that these rubs were essentially on an ingestion phenomena. It demonstrates, however, that the ingestion phenomena were caused by factors within the engine. The ingestion charges apparently were not due to interactions in the air streams prior to entering the compressor.

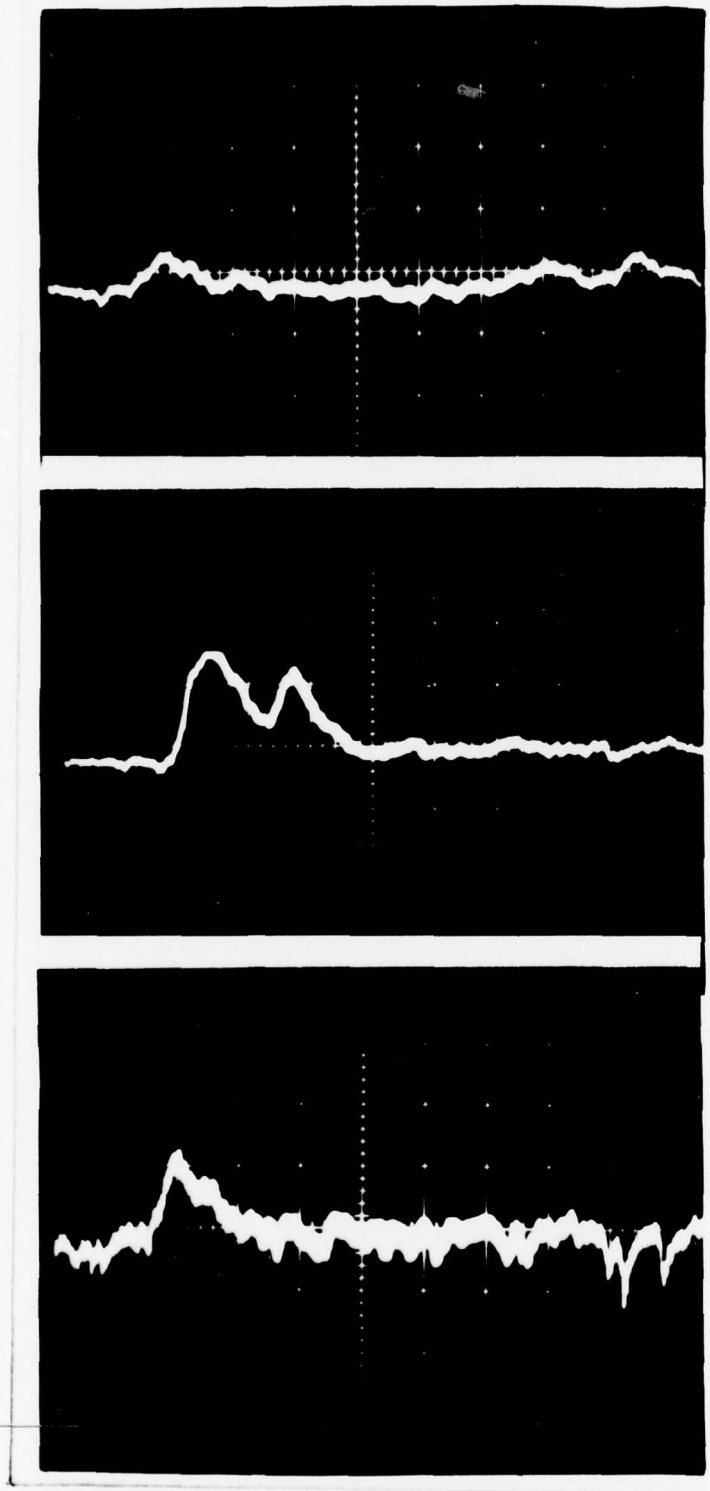

A.
Whole Body
(+ down)
2.0 S/cm
100 nanoamps/cm

B.
Whole Body
(+ down)
5.0 S/cm
22.0 nanoamps/cm

C.
Whole Body
(+ down)
2.0 S/cm
50 nanoamps/cm

Fig. 20 Whole Body Rub Distresses

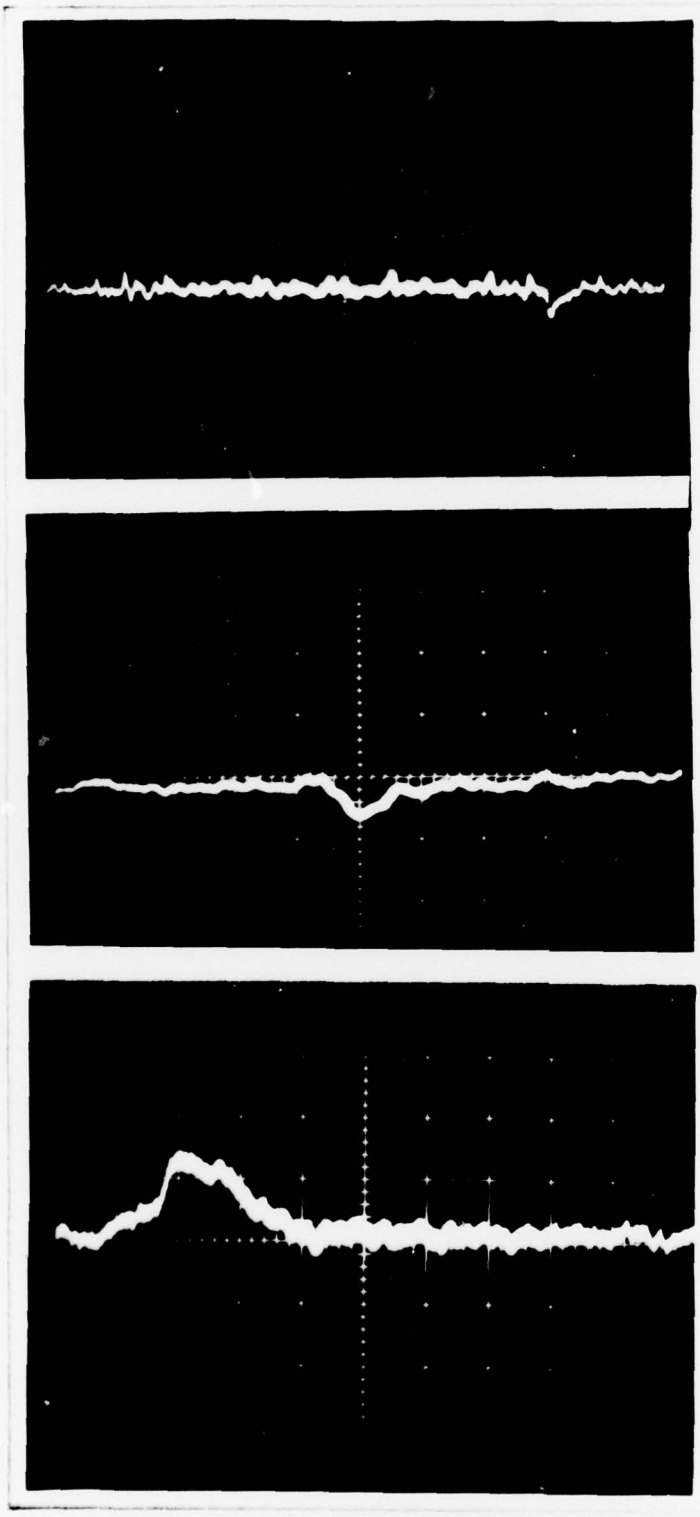

A.
King
(+ down)
0.5 S/cm
100 nanoamps/cm

B.
Probe
(+ down)
0.5 S/cm
5.0 nanoamps/cm

C.
Whole Body
Simulation
(+ down)
2.0 S/cm
100 nanoamps/cm

Fig. 21 Rub Distresses

Integration of the Ring Signal

An arbitrary amount of nickel was ingested in the engine. The whole body and ring signals were recorded on separate channels of the tape recorder. Pictures of these signals are displayed in Figures 22A and 22B.

The ring signal from the tape recorder was fed into the electrometer through a 5.1 megohm resistor. With the electrometer set on 0.1 microculombs, a capacitance of 0.1 microfarads was presented to the signal. This yielded an RC time constant of 0.5 seconds. Since this time constant was long compared to the ring signal duration, it integrated the signal. The output of the electrometer was fed directly into the storage scope. Figure 22C shows the integrated ring signal which is a mirror image of Figure 22A.

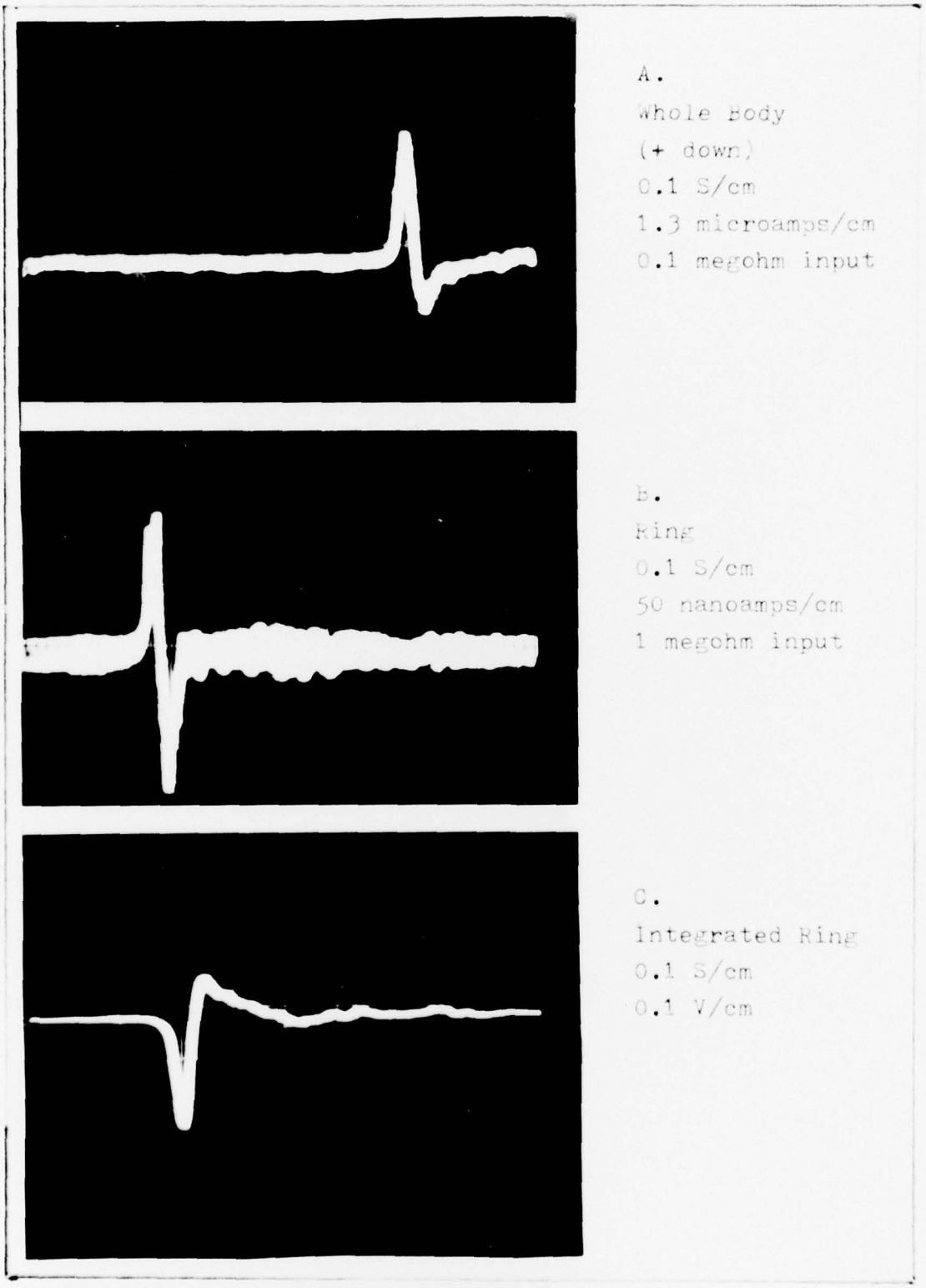

Fig. 22 Integration of the Ring Signal

V. Conclusions and Recommendations

Conclusions

The following observations are suggested by the experimental results. For 50 micron nickel powder ingestions of less than one gram, the charges observed are linearly dependent on two factors. These factors are the net charge (floating potential) in the exhaust prior to the ingestion and the amount of nickel ingested. Above one gram, the ingestion wave forms begin to develop a lower spike similar to that appearing in Figure 5. No attempt was made to obtain the ratio of the charge per mass for distresses producing a bipolar whole body wave form. The evidence suggests similar results can be expected for materials other than nickel powder.

Any charge leaving the exhaust must leave an equal and opposite charge on the engine frame. Therefore, the current between the chassis and ground when multiplied by the duration of the current flow yields the charge expelled. If the ratio of the charge to mass of the metal expelled in the exhaust is known, the total mass expelled from the engine can be estimated.

In many situations it is obviously impractical to measure the whole body current. However, electrical integration of the ring signal, as shown in a previous section, can reproduce the shape of the whole body current trace. The amplitude of the whole body trace is not provided by the integration of the ring signal. However, an analysis of a simultaneous recording of both the whole body current trace and the integrated ring trace can provide a proportionality constant correlating the two traces. With this constant the whole body current trace can be reconstructed from the ring signal. A measure of the total charge expelled

can then be provided by the ring trace alone. This approach eliminates the necessity both of having the engine frame isolated from ground and of having a measuring device connected from the engine frame to ground. Thus, the construction of an airborne system is feasible.

The probe and screen are less reliable than either the whole body detector or the ring. It is speculated that dynamic temperature, and contamination effects of the jet blast can alter their responses. Wide variances in signal wave forms were also observed when the impedance between the probe and ground was changed. However, by using the probe and screen in conjunction with the ring, overall reliability can be improved.

The polarity of the floating potential appears to determine the polarity of all distress wave forms including combustor can burns. However, this is a tentative conclusion. Negative floating potentials are observed only when the bleed valve is open. All the variables introduced by opening the bleed valve were not isolated nor were they all analyzed.

The following speculations are presented without conclusive evidence but are based on intuitive conclusions reached while performing the experiements. There are several charging mechanisms simultaneously working in the engine. The dominant mechanism is associated with the floating potential or excess ions in the exhaust. It is conjectured that the addition of small particles accelerates the removal of the more mobile ions or charges from the exhaust plasma. The accelerated transfer of charges from the plasma to the engine temporarily produces a higher net charge in the exhaust. In high temperature plasmas, Emeleus suggests that cold (temperature lower than the plasma) particles could be treated as insulated negative surface ionization sinks that add to the effect of the wall (Ref 5:1-18). Whether the same process is applicable to jet

engine plasma is uncertain. Candidates for the subordinate charging roles are diffusion charging, contact charging (particularly of insulators), and thermionic emission.

Calculations were performed relating the mass ingested to the amount of charge observed. A more realistic comparison is probably the ratio of the volume and/or surface area of the material ingested to the charge. Powdered graphite consistently produced approximately five times the charge of an equal mass of 50 micron powdered nickel. The density of nickel is approximately four times that of graphite. The graphite probably produced smaller particles on the average than those produced by the nickel powder. Thus the greater volume and smaller particles could account for graphite's consistently higher charge to mass ratio.

Considering titanium's density, the charge produced was less than anticipated. This suggests flammable or very hot particles may impede the charge transfer from a positive exhaust plasma. Since hot particles can thermionically emit electrons, this may tend to retard the electron or negative ion removal process.

Recommendations

Several experiments using the detection systems previously outlined are recommended in order to further study the changing mechanisms in a jet engine. These experiments are as follows:

1) The lack of uniform particle sizes made the charge comparisons between different materials difficult. Therefore, the use of accurately sized materials to study the effects of particle size versus charge produced for a variety of materials is suggested.

2) The use of various materials of different densities but of the same diameter to study the effect of material volume versus charge produced should be pursued.

3) Metals such as nickel, copper, titanium, and zirconium could be ingested in order to compare the effects introduced by ingesting a flammable material.

4) The placement of a small ring in the bleed air duct is strongly recommended. The bleed air is vented prior to the combustor can. A study of charges coming out of the bleed air duct versus those coming out the exhaust should give an insight into the effects of combustion. Lapple did an extensive literature review of the charging processes that would be germane to the bleed air measurement (Ref 9:1-95).

5) The ingestion of small quantities of lubricating oil to study the effects of liquid ingestions should be of interest.

6) Rubbing the turbine section of the MA-1A and comparing the results with compressor section rubs is another possibility.

7) An expanded comparison of the responses of insulators versus conductors should demonstrate the effects of contact charging. Insulators may pick up negative charges due to contact with the engine components and this could modify the signal response.

8) The final recommendation is that an engine such as a TF-41 be equipped with a ring and a probe or grid assembly. An ideal location for such a test would be at the depot overhaul facility at Tinker AFB, Oklahoma. Since numerous failures occur on engines coming out of depot maintenance, the reliability of using these systems could be firmly established.

Bibliography

1. Burgess, Ray W. An Investigation of the Detection of Charged Metal Particles in a Jet Engine Exhaust by a Cylindrical Electrostatic Probe. Thesis, AD745540, Wright-Patterson Air Force Base, Ohio: Air Force Institute of Technology, June 1972.

2. Couch, Robert P., et al. "Sensing Incipient Engine Failure." Progress in Astronautics and Aeronautics, 34:515-529 (1972).

3. Couch, R. P. The Use of Electrostatic Probes to Predict Jet Engine Failures. 1975 IEEE International Conference on Plasma Science, May 1975.

4. Couch R. P. and R. C. Poch. An Ion Probe to Predict Failures in Jet Engines. 8th Annual FAA International Aviation Maintenance Symposium, November 1974.

5. Emeleus, K. G. "Notes on the Effects of Dust in Positive Columns." International Journal of Electronics, 29:1-18 (1970).

6. Fowler, R. T. Ion Collection by an Electrostatic Probe in a Jet Exhaust. Thesis, AD874647, Wright-Patterson Air Force Base, Ohio: Air Force Institute of Technology, June 1970.

7. Hill, Gail E. Imminent Engine Failure Probe Investigation. AFAPL TR-74-30. Wright-Patterson Air Force Base, Ohio: Air Force Aero Propulsion Laboratory, 1974.

8. Kunkel, W. B. "The Static Electrification of Dust Particles on Disperson into a Cloud." Journal of Applied Physics, 21:820 (1950).

9. Lapple, C. E., et al. Advances in Chemical Engineering. New York: The Academic Press. 1970.

10. Loeb, L. B. Static Electrification. Berlin: Springer, 1958.

11. Mitchell, Donald A. and Mario Soliz. Evaluation of an Electrostatic Probe Technique for Detection of Turbine Engine Gas Path Distress, Comprehensive Summary Report. AFAPL TR-74-96. Wright-Patterson Air Force Base, Ohio: Air Force Aero Propulsion Laboratory, 1975.

12. -----, Evaluation of Electrostatic Probe Technique for Detection of Particles Emitted During Turbine Engine Distress. AFAPL TR-74-41. Wright-Patterson Air Force Base, Ohio: Air Force Aero Propulsion Laboratory, November 1974.

13. Mitchell, John E. Exploding Wire Simulation of Jet-Engine Gas-Path Microdistresses. Thesis, GNE/PH/75-20. Wright-Patterson Air Force Base, Ohio: Air Force Institute of Technology, December 1975.

14. Sajber, M., et al. Evaluation of Experiments Using Electrostatic Probes to Detect Imminent Failure of Jet-Engine Gas-Path Components. AFFDL TR-75-74. Wright-Patterson Air Force Base, Ohio: Air Force Flight Dynamics Laboratory, July 1975.

Appendix A

Supplementary Figures

This appendix contains supplementary figures to additionally illustrate the material presented in the body of this thesis.

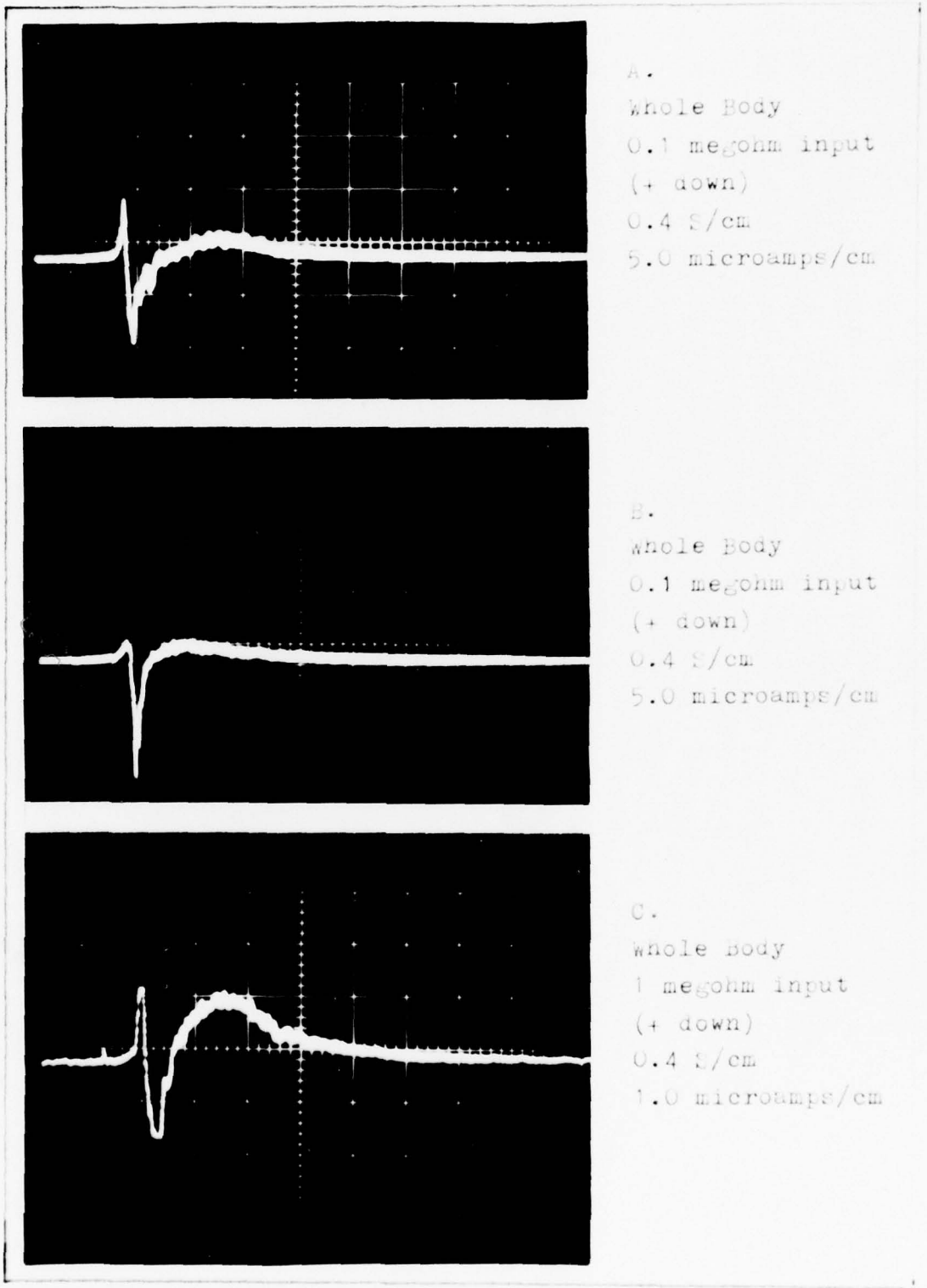

Fig. 23 Various Whole Body Ingestion Patterns 3 to 4 Grams Nickel

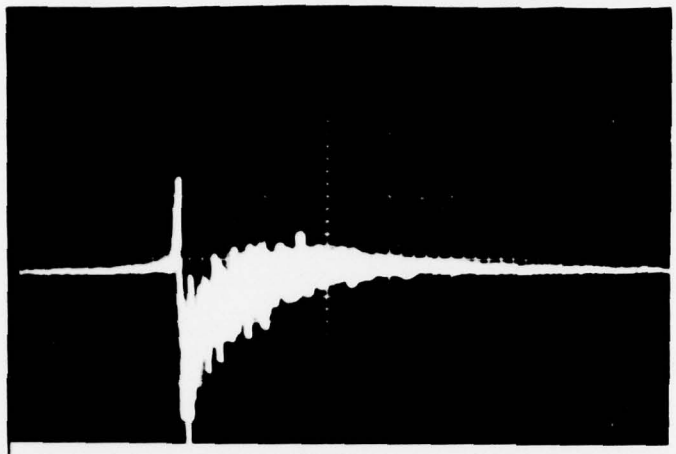

A.
Probe
1 megohm input
0.4 S/cm
100 nanoamps/cm

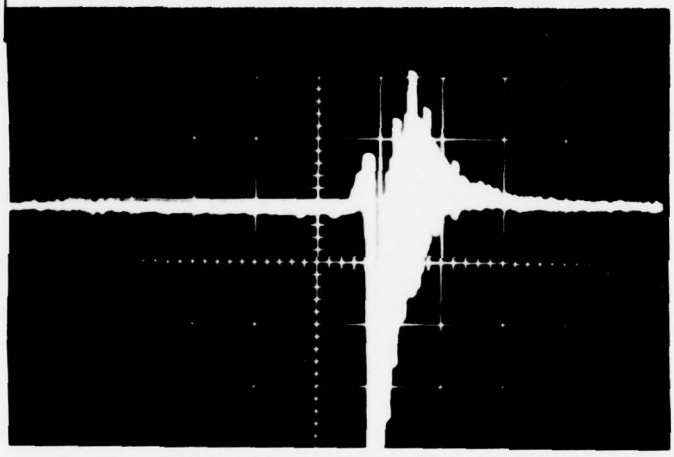

B.
Probe
1 megohm input
1.0 S/cm
50 nanoamps/cm

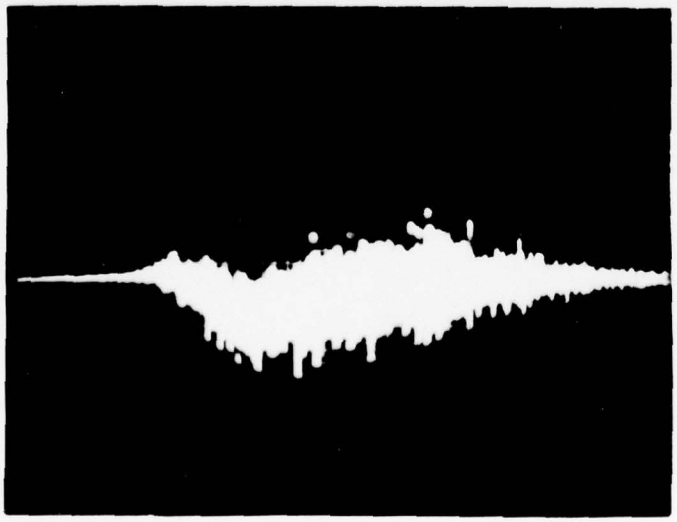

C.
Probe
0.1 megohm input
0.2 S/cm
200 nanoamps/cm

Fig. 24 Various Probe Ingestion Patterns
3 to 4 Grams of Nickel

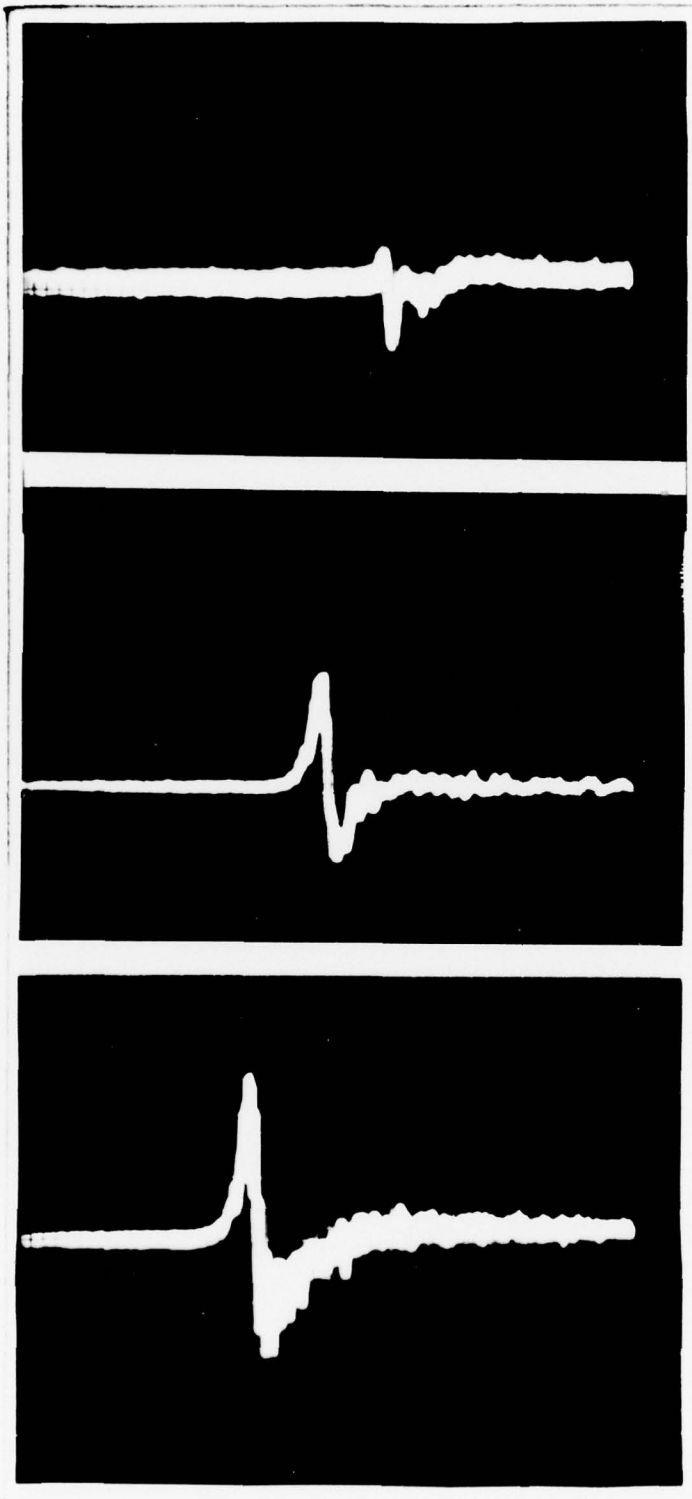

A.
Whole Body
(+ down)
0.5 S/cm
3 microamps/cm

B.
Ring
0.1 S/cm
0.1 microamps/cm

C.
Probe
0.1 S/cm
0.1 microamps/cm

Fig. 25 Nickel Ingestion 2 Grams Whole Body Input 100 Ohms (Same event A-C)

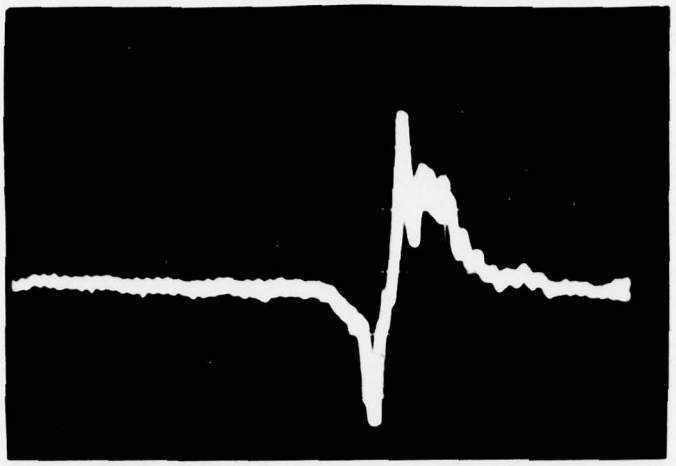

A.
Whole Body
(+ down)
0.1 S/cm
0.3 microamps/cm

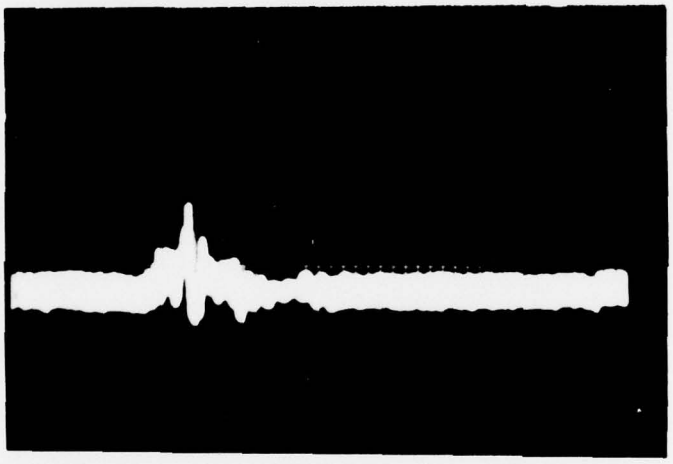

B.
Ring
0.1 S/cm
50 nanoamps/cm

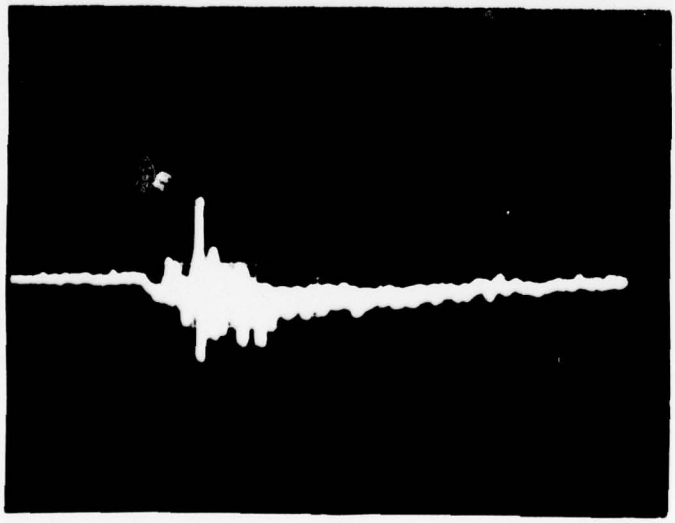

C.
Probe
0.1 S/cm
100 nanoamps/cm

Fig. 26 Nickel Ingestion
Negative Plasma

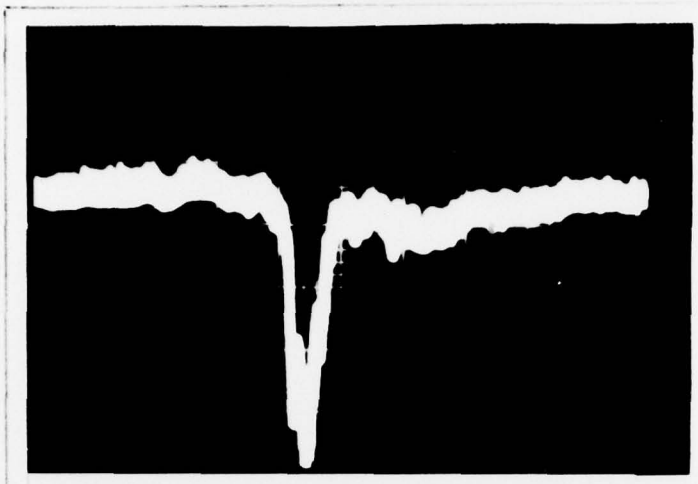

A.
Whole Body
(+ down)
0.2 S/cm
0.13 microamps/cm
Titanium

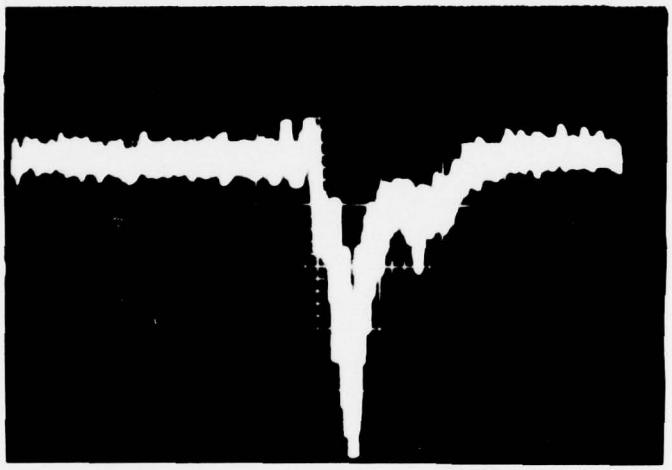

B.
Probe
0.2 S/cm
20 nanoamps/cm
Titanium
Same event as A

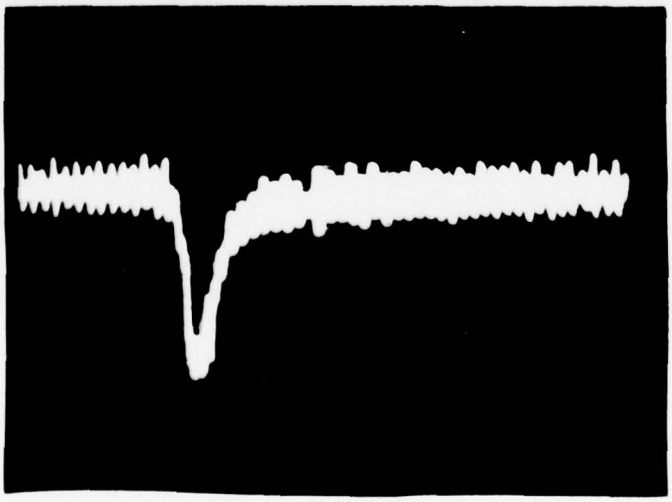

C.
Whole Body
(+ down)
0.2 S/cm
3.3 microamps/cm
Quartz

Fig. 27 Negative Plasma Ingestions

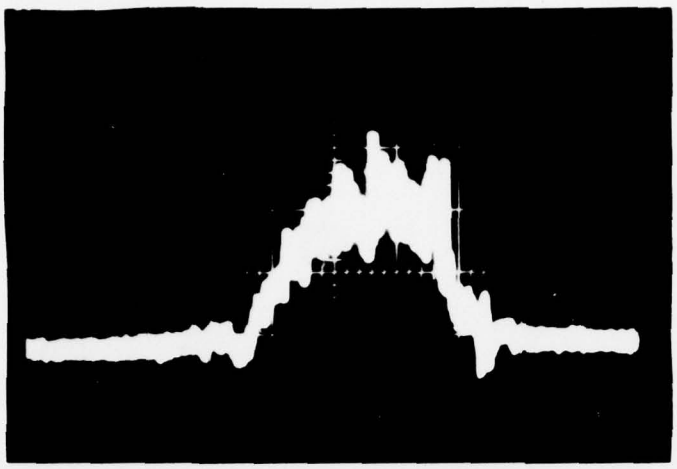

A.
Whole Body
(+ down)
1 S/cm
0.33 microamps/cm

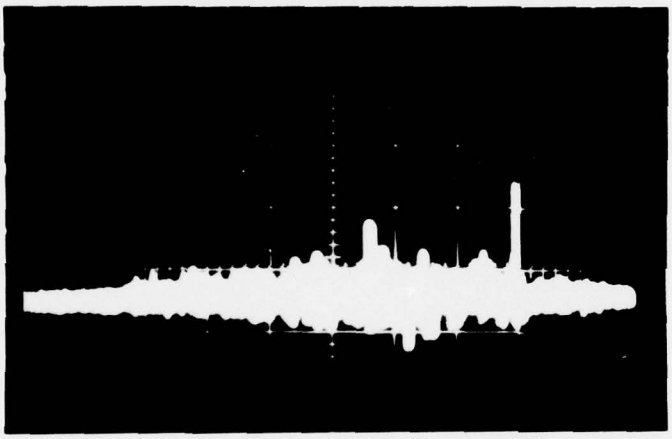

B.
Ring
0.5 S/cm
50 nanoamps/cm

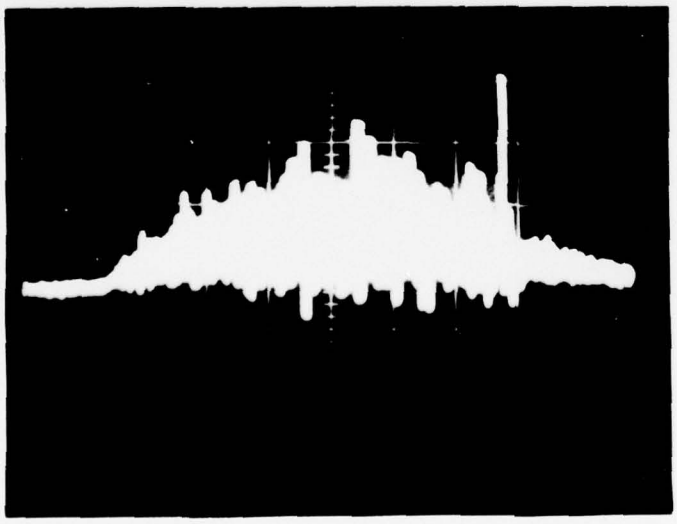

C.
Probe
0.5 S/cm
50 nanoamps/cm

Fig. 28 Ingestion 37 Micron Nickel
Eye Dropper (Same events)

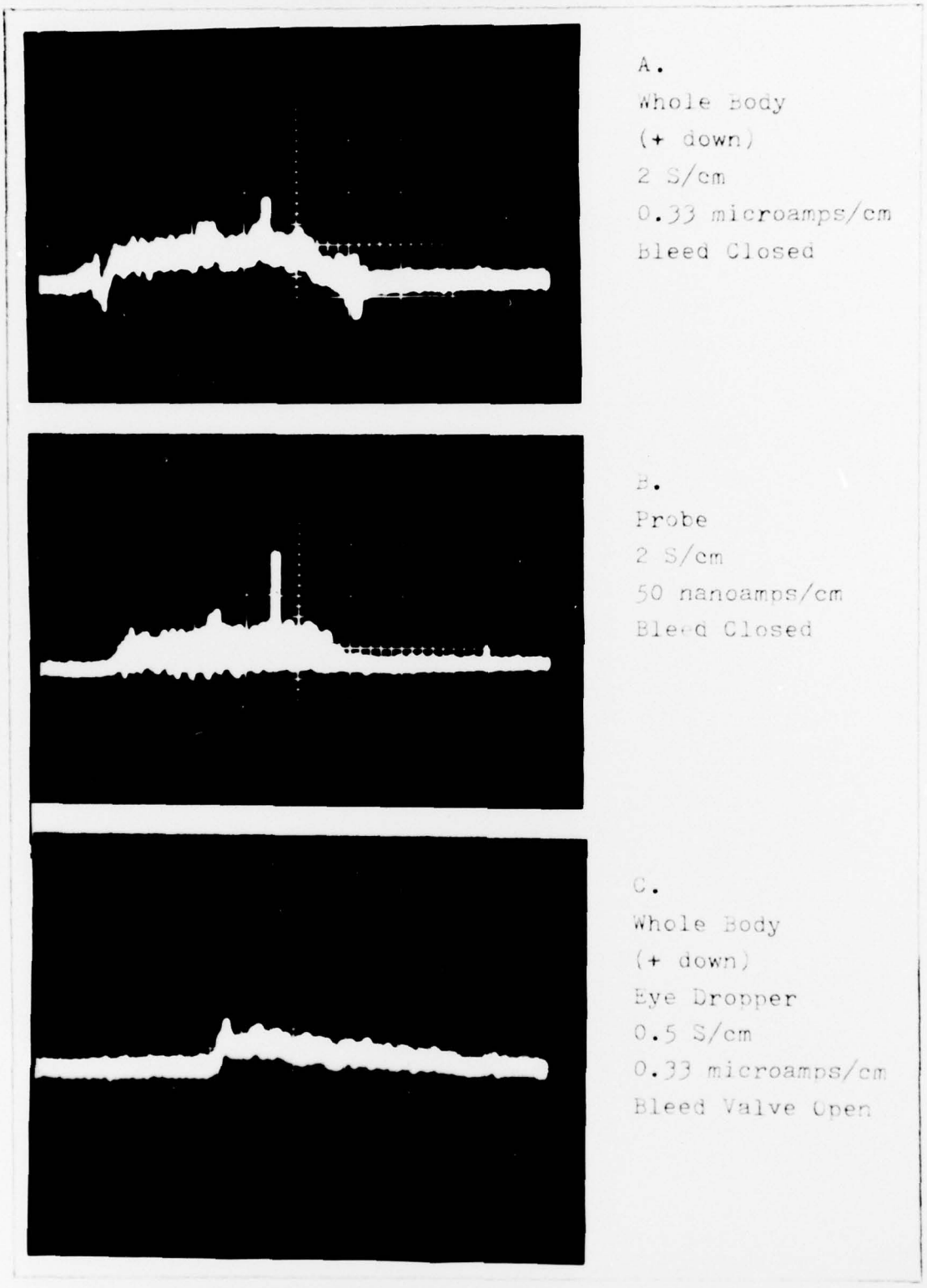

Fig. 29 Positive Plasma 37 Micron Nickel
(Flow Rate in C Faster than A)

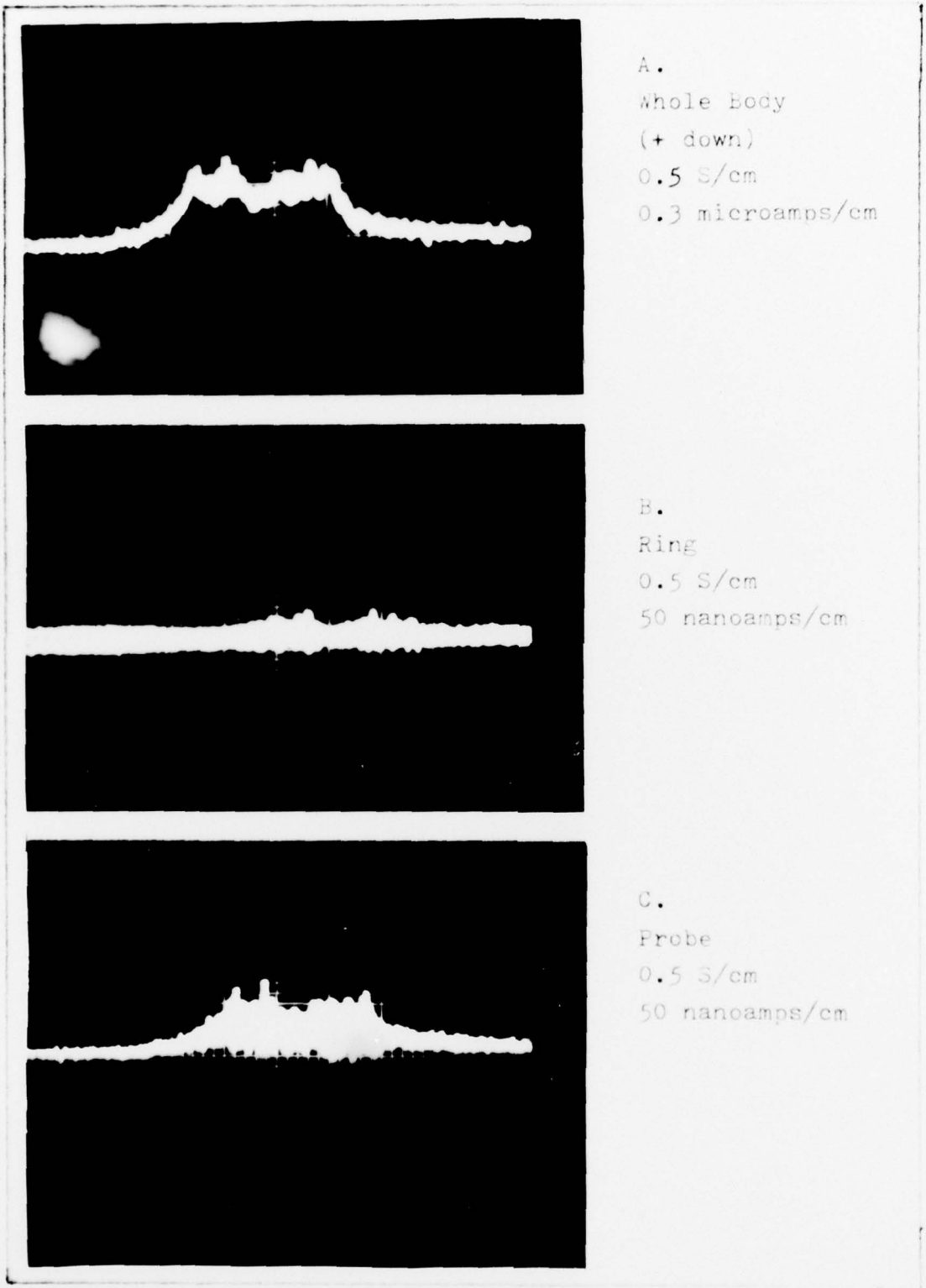

Fig. 30 Quartz Ingestion Using Eye Dropper Bleed Closed

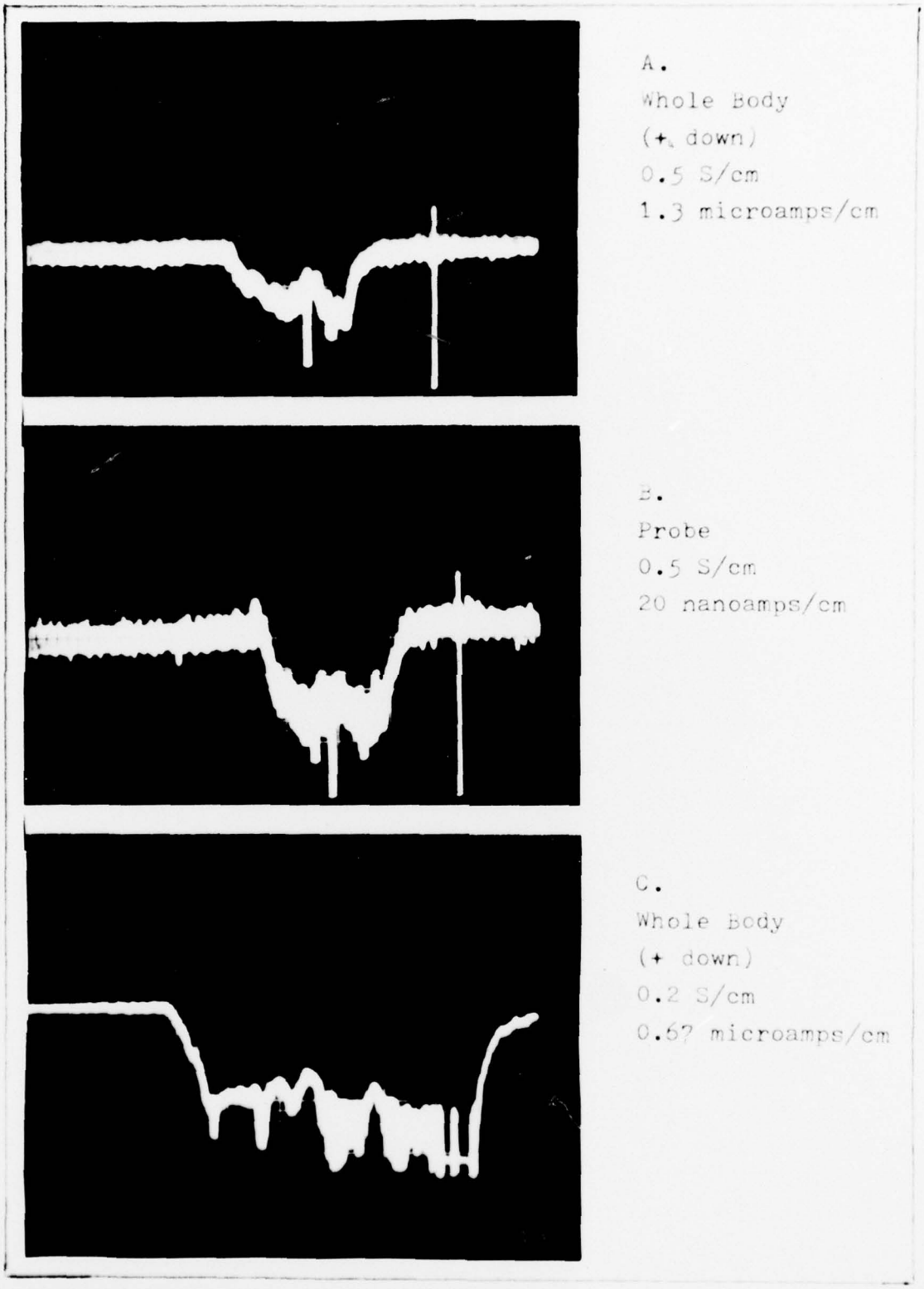

Fig. 31 Quartz Ingestion Bleed Open

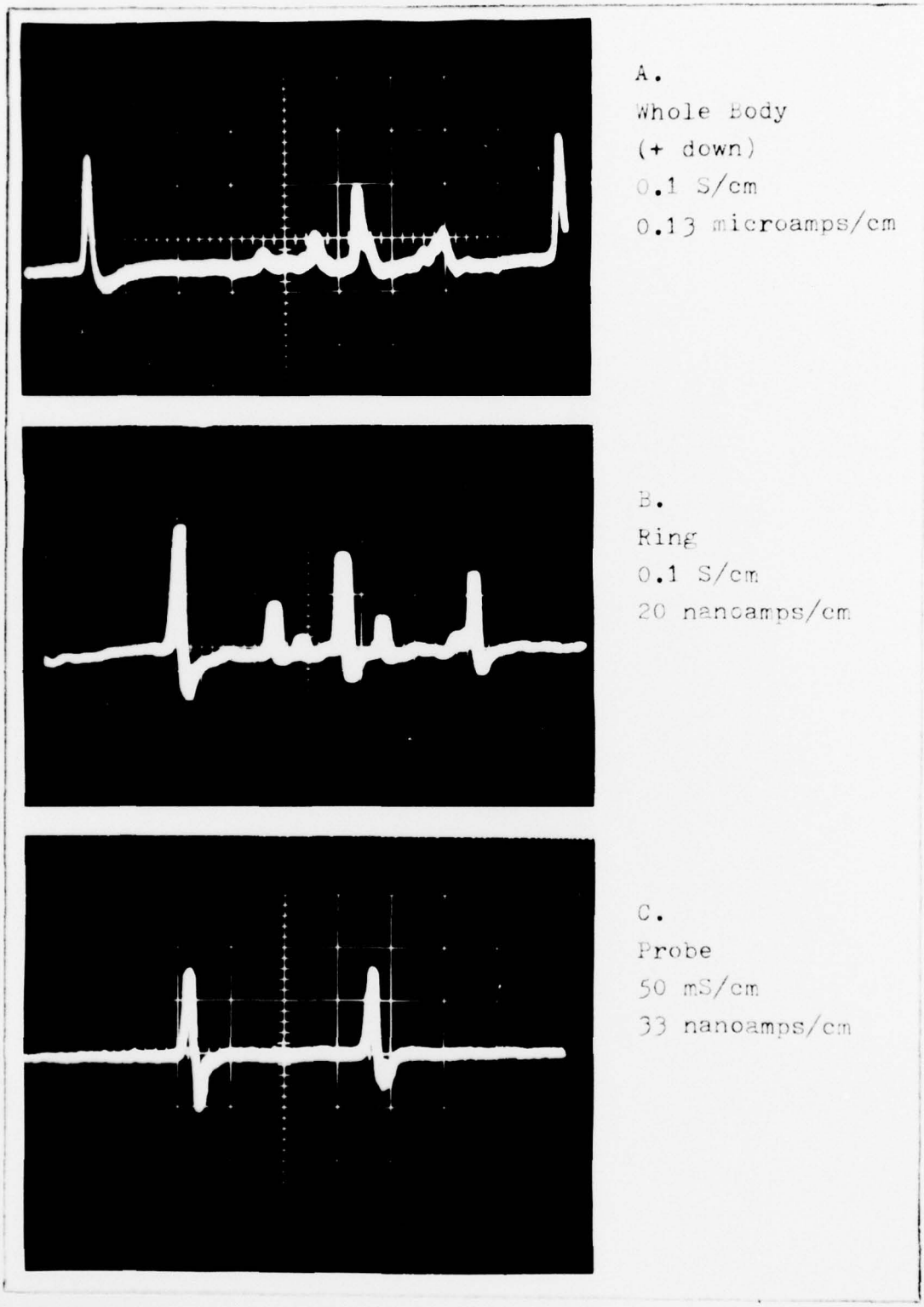

Fig. 32 Magnesium Burn

Appendix B

The Screen Detection System

The screen was placed in the exhaust blast to demonstrate that such a system would respond to charges emitted from an engine. It was located 42 inches above the exhaust outlet. A detection device such as a screen does not have to be an integral part of the engine and can be located a reasonable distance from the exhaust nozzle.

A detailed examination of the screen response patterns was not made. The response of the screen appears to be a cross between a ring and a probe.

Figure 33A shows the trace created by the ingestion of two to three grams of 50 micron nickel powder. The ingestion of a 47 milligram buck-shot is shown in Figure 33B. Figure 33C demonsrates the pattern caused by aluminum oxide. Figures 34A and 34B show the patterns established by ingesting flour and graphite. A magnesium burn in the combustor can is shown in Figure 34C.

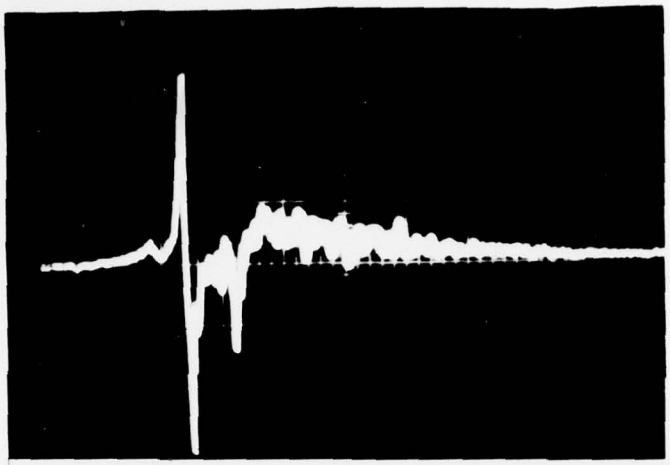

A.
Screen
0.4 S/cm
100 nanoamps/cm

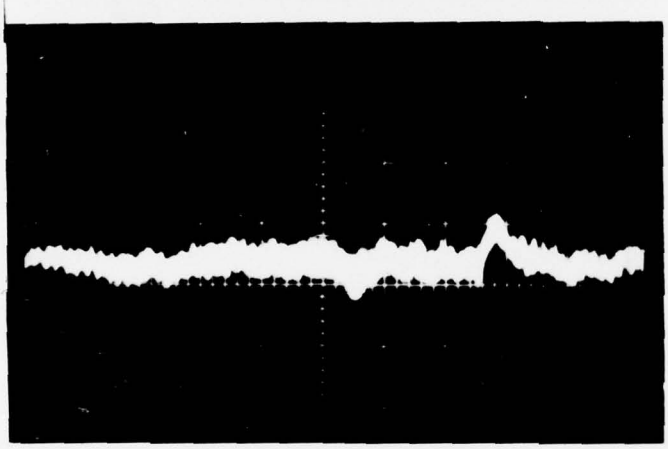

B.
Screen
0.1 S/cm
50 nanoamps/cm

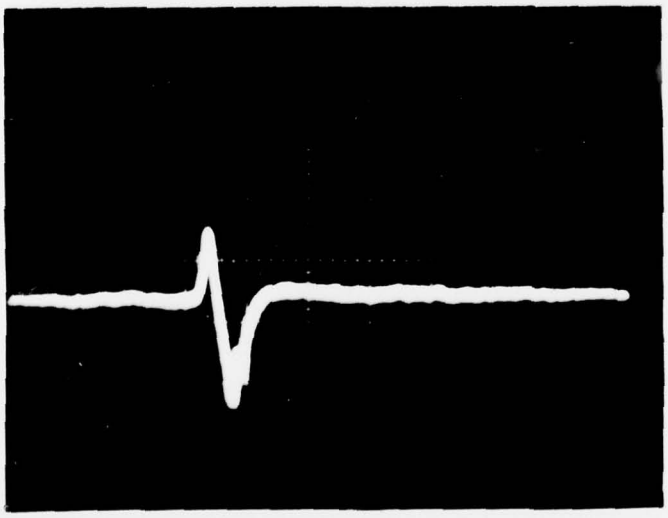

C.
Screen
0.2 S/cm
250 nanoamps/cm

Fig. 33 Screen Ingestion Nickel, Buckshot, and Aluminum Oxide

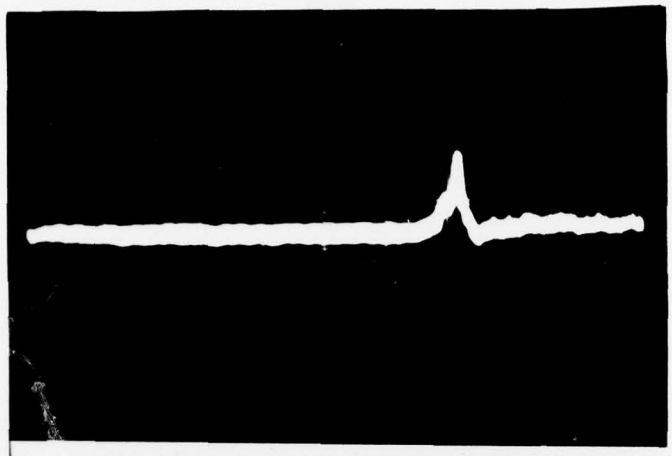

A.
Screen flour
0.2 s/cm
250.0 nanoamps/cm

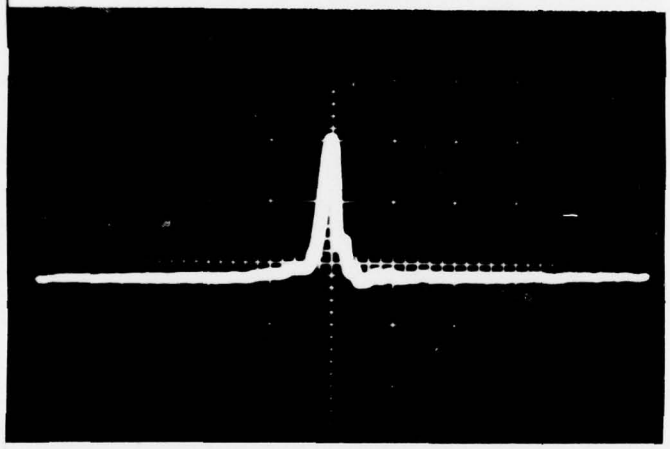

B.
Screen graphite
0.2 s/cm
50.0 nanoamps/cm

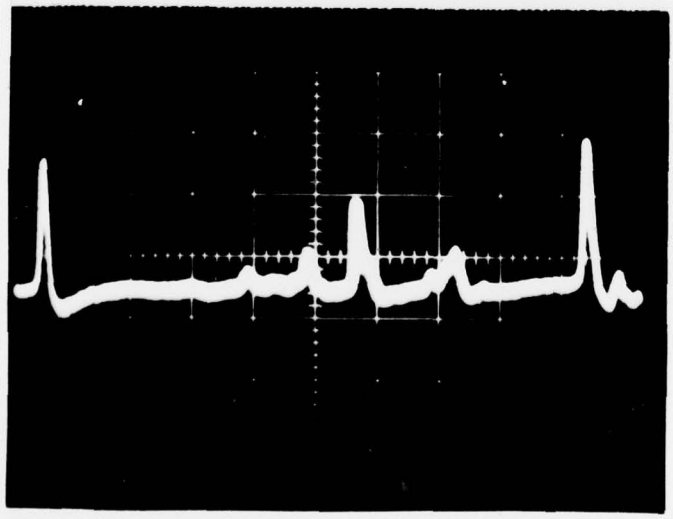

C.
Screen magnesium
0.1 s/cm
200.0 nanoamps/cm

Fig. 34 Screen Wave Forms

Appendix C

Charge Calculations

The method used to compute the charges was to tape the whole body current traces at a high tape recorder speed. The recorder was then slowed down to an appropriate speed and a picture from the oscilloscope was taken. The area under the curve was calculated using the approach formulated by Mitchell (Ref 13:21).

The area of the photograph is given in units of voltseconds. The calculations are performed as follows:

$$V = IR$$

where R = input impedance

$$I = V/R$$

$$Q/t = V/R$$

$$Q = Vt/R$$

where Vt is in units of voltseconds.

Table I contains some order of magnitude charge to mass ratios for several materials and types of distresses. The calculations were made by dividing the calculated charge by the mass of the material injected into the gas flow. The chassis current was approximately 10 to 15 nanoamperes when these measurements were made.

Figure 35 shows a graph of 50 micron nickel charge per mass ratios plotted against the quiescent whole body or chassis current. The ingestions were all under one gram to preclude a bipolar wave form. Also, the whole body current only varied a maximum of 20 nanoamperes. Within the

Table 1

Charge per Mass in

Nanocoulombs/Milligram

Material	Charge	Distress
Magnesium Strip	1.4	Burn
Aluminum-Magnesium Rod	0.4	Burn
Aluminum Wire	0.2	Burn
Quartz	0.2	Ingestion
Nickel 50 Micron	0.4	Ingestion
Aluminum Oxide	0.4	Ingestion
Titanium	0.5	Ingestion
Flour	1.2	Ingestion
Graphite	2.0	Ingestion

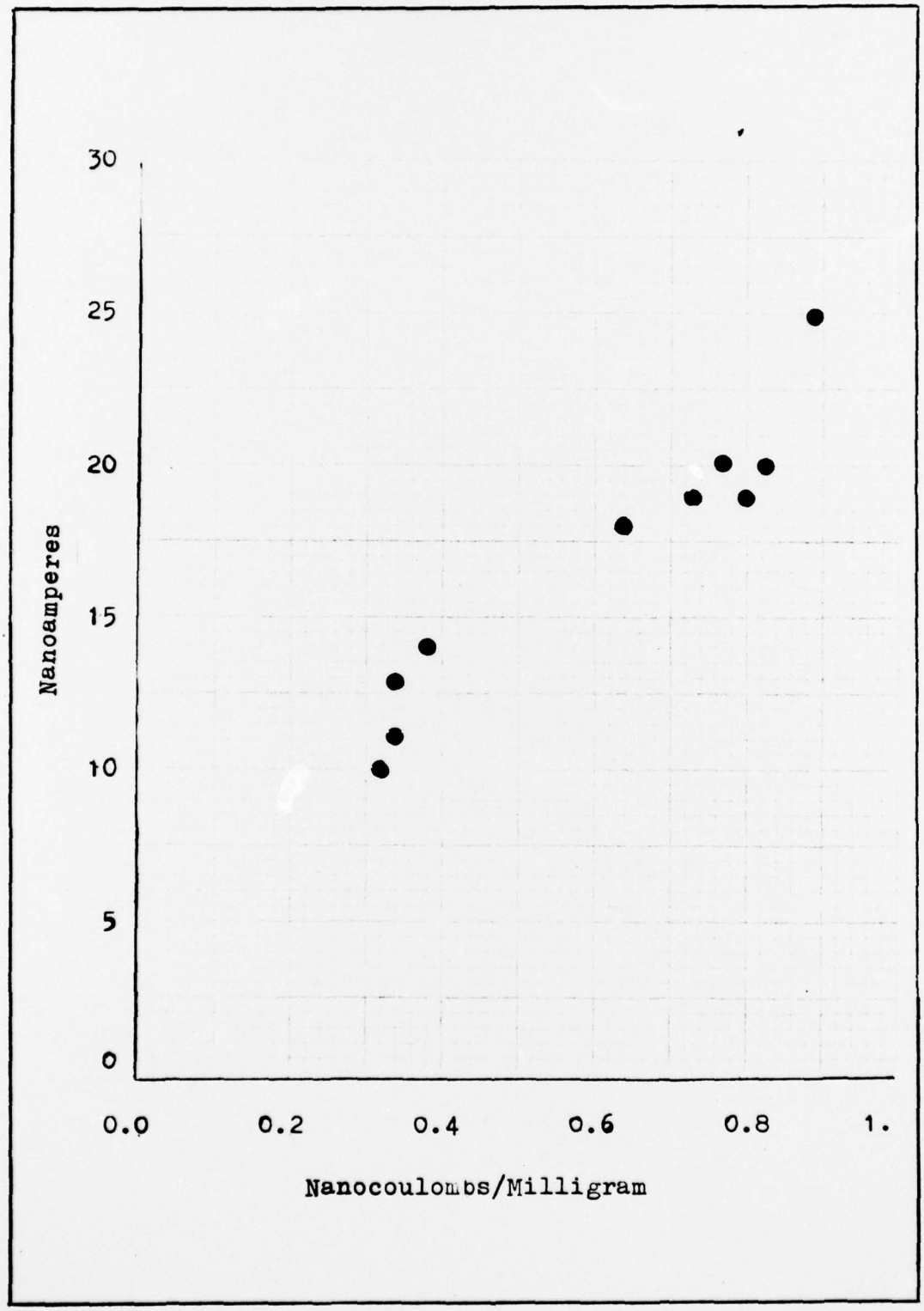

Fig. 35 Charge/Mass Versus Chassis Current

above ranges the charge to mass ratios of nickel appear to vary linearly with the whole body current. The whole body current was measured immediately before the ingestion.

VITA

Robert Wesley Dunn was born on 9 January 1943 in Monroe, Michigan. In 1961 he graduated from University High School in Waco, Texas. In 1965 he received the degree of Bachelor of Science in Secondary Education from the University of Texas at Austin. He taught in the Texas public school system until entering the Air Force in 1968. His first two assignments were as an Avionics maintenance officer at McQuire Air Force Base, New Jersey, and then at Charleston Air Force Base, South Carolina. Prior to entering the School of Engineering, Air Force Institute of Technology in June 1975, he was assigned as an instructor at Officer Training School at Lackland Air Force Base, Texas.

Permanent address: 2811 Old Robinson Road
Waco, Texas 76706

This thesis was typed by Ms. Carmma G. Troxell.

UNCLASSIFIED
SECURITY CLASSIFICATION OF THIS PAGE (When Data Entered)

REPORT DOCUMENTATION PAGE		READ INSTRUCTIONS BEFORE COMPLETING FORM
1. REPORT NUMBER GNE/PH/76-2	2. GOVT ACCESSION NO.	3. RECIPIENT'S CATALOG NUMBER
4. TITLE (and Subtitle) THE ELECTROSTATIC SENSING OF SIMULATED MA-1A GAS PATH DISTRESSES		5. TYPE OF REPORT & PERIOD COVERED MS THESIS 6. PERFORMING ORG. REPORT NUMBER
7. AUTHOR(s) ROBERT W. DUNN Capt USAF		8. CONTRACT OR GRANT NUMBER(s)
9. PERFORMING ORGANIZATION NAME AND ADDRESS Air Force Institute of Technology (AFIT/EN) Wright-Patterson AFB, Ohio 45433		10. PROGRAM ELEMENT, PROJECT, TASK AREA & WORK UNIT NUMBERS
11. CONTROLLING OFFICE NAME AND ADDRESS Air Force Institute of Technology (AFIT/EN) Wright-Patterson AFB, Ohio 45433		12. REPORT DATE December 1976 13. NUMBER OF PAGES 74
14. MONITORING AGENCY NAME & ADDRESS(if different from Controlling Office)		15. SECURITY CLASS. (of this report) UNCLASSIFIED 15a. DECLASSIFICATION/DOWNGRADING SCHEDULE

16. DISTRIBUTION STATEMENT (of this Report)

Approved for public release; distribution unlimited

17. DISTRIBUTION STATEMENT (of the abstract entered in Block 20, if different from Report)

18. SUPPLEMENTARY NOTES

Approved for public release; IAW AFR 190-17
JERRAL F. GUESS, Captain, USAF
Director of Information

19. KEY WORDS (Continue on reverse side if necessary and identify by block number)

Electrostatic
Ion Probe
MA-1A
Gas Path Distress

20. ABSTRACT (Continue on reverse side if necessary and identify by block number)

Jet engine distresses were simulated using a MA-1A start cart. Three primary methods were used to distress the gas turbine engine. Material was ingested through the compressor intake, the compressor section was rubbed with an aluminum rod, and foreign material was burned in the combustor can.

The current wave forms created by these distresses were observed with four separate detectors. Since the MA-1A was on rubber tires, the current between the chassis and ground could be measured. This chassis current was equal

DD FORM 1 JAN 73 1473 EDITION OF 1 NOV 65 IS OBSOLETE

UNCLASSIFIED
SECURITY CLASSIFICATION OF THIS PAGE (When Data Entered)

to the rate at which charge was expelled in the exhaust. A Gaussian ring around the exhaust port provided a second way of detecting charges leaving the start cart. The third and fourth devices were an ion probe and a screen that were placed in the exhaust.

It was found that the ring current was proportional to the derivative of the chassis current. The charges recorded by these detectors were noted to be dependent on the net charge present in the exhaust prior to distress. The charges were also dependent on the amount of material introduced by the distress.